



An improved adaptive hybrid firefly differential evolution algorithm for passive target localization

Maja B. Rosić¹ · Mirjana I. Simić¹ · Predrag V. Pejović¹

Published online: 13 January 2021

© The Author(s), under exclusive licence to Springer-Verlag GmbH, DE part of Springer Nature 2021

Abstract

This paper considers a passive target localization problem based on the noisy time of arrival measurements obtained from multiple receivers and a single transmitter. The maximum likelihood (ML) estimator for this localization problem is formulated as a highly nonlinear and non-convex optimization problem, where conventional optimization methods are not suitable for solving such a problem. Consequently, this paper proposes an improved adaptive hybrid firefly differential evolution (AHFADE) algorithm, based on hybridization of firefly algorithm (FA) and differential evolution (DE) algorithm to estimate the unknown position of the target. The proposed AHFADE algorithm dynamically adjusts the control parameters, thus maintaining high population diversity during the evolution process. This paper aims to improve the accuracy of the global optimal solution by incorporating evolutionary operators of the DE in different searching stages of the FA. In this regard, an adaptive parameter is employed to select an appropriate mutation operator for achieving a proper balance between global exploration and local exploitation. In order to efficiently solve the ML estimation problem, this paper proposes the well-known semidefinite programming (SDP) method to convert the non-convex problem into a convex one. The simulation results obtained from the proposed AHFADE algorithm and well-known algorithms, such as SDP, DE and FA, are compared against Cramér–Rao lower bound (CRLB). The statistical analysis has been performed to compare the performance of the proposed AHFADE algorithm with several well-known algorithms on CEC2014 benchmark problems. The obtained simulation results show that the proposed AHFADE algorithm is more robust in high-noise environments compared to existing algorithms.

Keywords Localization · Time of arrival · Firefly algorithm · Differential evolution · Hybrid optimization · Cramér–Rao lower bound

1 Introduction

The problem of finding the position of passive target based on noisy TOA measurements is an essential task that has received extensive attention in various applications, such as radar, wireless communications, navigation, environmental monitoring, biomedical health monitoring (Wu et al. 2016; Deak et al. 2012; Sachs 2013), etc. In general, depending on the nature of the target to be determined, localization systems can be classified into active and passive, based on the target's participation in the localization process (Deak et al. 2012). In the active localization, the target actively participates in the localization process. Unlike active localization systems, in

passive localization systems, the target is not involved in the localization process. The passive localization aims to determine the position of the target without any device or tag; in fact, the target can only reflect or scatter the signals from transmitter to receivers (Wu et al. 2016).

Generally, the global positioning system (GPS) and other similar global navigation satellite systems provide access for obtaining the exact position of an object anywhere on the Earth surface (Yan et al. 2018). However, their positioning accuracy is not satisfactory due to the restriction of signal arrival in special environments, such as indoor, urban and underwater acoustics, and therefore, other solutions are required for target localization (Choi et al. 2014; Noroozi and Sebt 2015). In this context, the passive localization system is one of the widely used systems to estimate the unknown position of the target, due to its ability to achieve very high localization accuracy. Hence, this paper considers the passive target localization problem using noisy TOA

✉ Maja B. Rosić
rosic.maja9@gmail.com

¹ University of Belgrade School of Electrical Engineering,
Bulevar kralja Aleksandra 73, Belgrade, RS, Serbia

measurements, as the sum of the signal propagation time from the known position of the transmitter to the target with unknown position, and that from the target to each receiver with known position. In this case, the signal propagation time can be measured and used to estimate ranges (transmitter–target–receiver distances). In fact, the obtained noisy distance measurements are nonlinear with respect to the unknown position of the target. Hence, the sum of transmitter–target and target–receiver ranges defines an ellipse. In this way, the estimated position of the passive target can be found inside the region bounded by the corresponding ellipses. In this context, the estimation of the target position is one of the most challenging optimization problems, which in recent years has become of practical significance (Chalise et al. 2014). In the line-of-sight (LOS) environment, the TOA measurement errors can be modeled as Gaussian distributed random variables. Therefore, the ML estimator which is based on an a priori statistical information of the measurement error by maximizing the likelihood function, can be employed in order to obtain the unknown target position (Wang et al. 2014). The corresponding ML objective function for the given localization problem is a highly nonlinear and non-convex function, where conventional optimization methods are not suitable for solving such a problem. Consequently, this has motivated the development of different efficient optimization methods, which can accurately solve the ML estimation problem. Among them, the SDP has gained considerable attention as an efficient method that can be used to solve convex relaxations for the given localization problem (Chalise et al. 2014). The basic idea of the SDP method is to transform the non-convex problem to a convex one that monotonically converges to the global optimal solution. The main advantage of the SDP method is that it does not require an initial guess at the beginning of the optimization process, and in this way, the global optimal solution of the ML objective function can be efficiently found (Chan et al. 2013). In fact, the SDP method has received significant attention due to its numerical reliability and robustness in solving a variety of localization problems. The SDP problem can be efficiently solved using the MATLAB package CVX, where the solver is SeDuMi (Grant and Boyd 2014). However, the SDP method has some disadvantages in the presence of significant measurement noise, which is reflected in the accuracy of the global optimal solution, and thus, it cannot provide high estimation accuracy (Wang et al. 2013). In view of this, the problem of finding the global optimal solution with high accuracy for the multimodal objective function becomes a significant challenge.

Motivated by these facts, this paper proposes evolutionary algorithms (EAs) to overcome these drawbacks in finding the global optimal solution for a given multimodal optimization problem (Zhang et al. 2016). Generally, the evolution process of EAs consists of two stages, namely global exploration and

local exploitation, which have the crucial role for the performance of the algorithm (Mohamed and Almazayad 2017). In such a context, the exploration stage refers to search for the global solution, while the exploitation stage concentrates on the promising area to refine the solution around the current global best solution. Hence, finding an appropriate balance between exploration and exploitation of the search space is an important challenge for the optimization algorithm.

Various EAs have been successfully applied to solve complex optimization problems, such as genetic algorithm (GA) (Kuila et al. 2013), DE (Storn and Price 1997), FA (Wu et al. 2019), cuckoo search algorithm (CSA) (Goyal and Patterh 2014), particle swarm optimization (PSO) (Zhang et al. 2015b), etc. Among the various existing algorithms, the DE and FA have been widely applied for different multimodal optimization problems, due to their compact structure, easy implementation, reliability and robustness (Wu et al. 2019, 2018).

The FA is nature-inspired metaheuristic algorithm, which is based on the flashing behavior of fireflies. The search process of FA depends on the attraction of fireflies, whereby a less bright firefly moves toward a brighter firefly (Yang 2010b). Hence, the characteristics of the flashing light of fireflies provide effective diversity in searching for the global optimal solution. In this regard, the objective function for a given optimization problem is associated with the light intensity. The FA has been successfully employed to solve different complex optimization problems, and it has shown its superiority in comparison with the optimization performance of well-known algorithms, such as GA and PSO (Yang 2009). Similar to other EAs, the FA has some drawbacks, such as premature convergence to a local optimum, slow convergence rate, especially in the later stage of the evolution process, and sensitivity to the choice of control parameters (Wang et al. 2017).

The hybridization of FA with other metaheuristic algorithms has been performed, in order to overcome drawbacks of conventional algorithms, which results in a powerful and highly effective optimization algorithm. For this purpose, the simulated annealing (SA) has been hybridized with FA into hybrid SFA, with the aim to improve the accuracy of the global optimal solution during the evolution process (Alweshah and Abdullah 2015). Moreover, to control the randomization movement of the FA, the crossover and mutation operators of GA have been integrated into the FA, which has increased convergence speed (Luthra and Pal 2011). There are also different hybrid variants of the FA with other metaheuristic methods, such as hybrid FA with DE (AHEFA) (Lieu et al. 2018), FA with PSO (HFPSO) (Aydilek 2018), FA with harmony search (HS/FA) (Guo et al. 2013) and FA with ant colony optimization algorithm (HAFA) (Goel and Maini 2018), which are very robust in finding global optimal solutions. Therefore, hybridization of these algorithms

has been successfully applied to solve various complex optimization problems, due to their effectiveness, improvement of convergence speed and solution accuracy, and the ability to avoid being trapped in local minima.

The DE is another population-based stochastic algorithm, developed by Storn and Price (Storn and Price 1997), that can be used for solving numerous optimization problems in different fields of science and engineering (Baraldi et al. 2016; Awad et al. 2018). The performance of the DE algorithm is significantly influenced by its control parameters, such as scale factor (F), crossover rate (CR) and population size (NP), and trial vector generation operators, i.e., mutation and crossover operators (Cui et al. 2016). In the DE algorithm, the values of the control parameters are kept fixed throughout the evolution process, which may cause the algorithm to be easily trapped in local optima of a multimodal objective function. Therefore, in order to improve the search performance of DE algorithm, many different mechanisms have been introduced to adjust control parameters in an adaptive or self-adaptive manner (Das et al. 2016). Among them, the JADE is a well-known DE variant with an effective parameter adaptation technique, where control parameters F and CR, associated with each individual in the population, are randomly and independently generated according to Cauchy and Gaussian distributions, respectively (Zhang and Sanderson 2009). Their expected mean values are adaptively updated using the successful values of F and CR during the evolution process to maintain diversity of the population and improve the robustness of the algorithm. Building on the success of JADE, the SHADE is proposed as the improved success history-based parameter adaptation technique, where the values of F and CR are adapted based on learning from successes and failures of past generations to accurately locate the global optimum (Tanabe and Fukunaga 2013).

Besides the control parameters, the mutation operator plays an important role in the evolution process of the DE algorithm. Various mutation operators have been suggested in the literature, such as DE/rand/1, DE/rand/2, DE/best/1, DE/best/2, DE/current-to-best/1, DE/current-to-rand/1 and other variants of them (Mohamed and Suganthan 2018). In addition, in the JADE algorithm, an effective mutation operator DE/current-to-pbest/1 is developed by improving the classic DE/current-to-best/1 operator (Zhang and Sanderson 2009). More recently, in composite DE (CoDE), a new mutation operator is proposed, which combines three trial vector generation strategies, such as DE/rand/1/bin/, DE/rand/2/bin, DE/current-to-rand/1, and three control parameter settings to generate trial vectors (Wang et al. 2011). In this regard, in order to achieve a proper balance between exploration and exploitation abilities, the mutation operator cannot be the same at different stages of the evolution process (Qian et al. 2018).

Motivated by the above considerations, in this paper, an improved adaptive hybrid algorithm, based on hybridization of the DE and FA, named AHFADE, is presented in order to efficiently solve the passive target localization problem. This paper aims to maintain population diversity and improve the convergence speed by incorporating evolutionary operators of the DE into the FA. To further improve the optimization performance, the control parameters of DE and FA are automatically and adaptively updated during the evolution process, where parameters F and CR are generated using Cauchy and Gaussian distributions, respectively. In addition, the proposed AHFADE algorithm incorporates two mutation operators DE/rand/1 and DE/current-to-pbest/1 into the FA to achieve an effective trade-off between exploration and exploitation abilities. Therefore, the purpose of this paper is to develop a robust optimization algorithm to solve the passive target localization problem for a wide range of measurement noise.

The CRLB is an important and widely applied in the localization for the analysis of the accuracy of the estimated target position, which provides a lower bound for the root mean square error (RMSE) of any unbiased estimator (Shen et al. 2012). Hence, the CRLB for the passive target localization problem is compared with the RMSE performance of the proposed AHFADE algorithm and the existing SDP, DE and FA.

The main contributions of this paper are summarized as follows:

- The passive target localization problem is defined in two dimensions based on the noisy TOA measurements obtained from a single transmitter and multiple receivers in LOS environment. Since the ML objective function of this localization problem is a highly nonlinear and non-convex function, it is necessary to provide sophisticated optimization algorithms, to estimate the position of the target.
- In order to efficiently solve the above ML estimation problem, the well-known SDP method can be employed to transform the non-convex optimization problem into a convex problem.
- The improved AHFADE algorithm, as a hybridization of the DE and FA, is established to provide desirable accuracy in LOS environment. The proposed AHFADE algorithm aims to improve the accuracy of the global optimal solution by incorporating evolutionary operators of the DE into the FA. Furthermore, the control parameters of the proposed AHFADE algorithm have been dynamically updated at each iteration to generate potential solutions with higher diversity.
- The statistical analysis using the Wilcoxon signed-rank test and Friedman test has been performed, in order to compare the performance of the proposed AHFADE

algorithm to several well-known algorithms on CEC2014 benchmark test problems. The obtained results further confirmed that the hybridization proposed in this paper can improve the overall optimization performance of the proposed AHFADE algorithm.

- The obtained numerical simulation results have shown that the AHFADE algorithm achieves the CRLB and has significantly better performance than existing algorithms. Furthermore, the simulation results indicate that the AHFADE is robust against large measurement noise and changes in the geometric configuration of the transmitter, target and receivers compared to SDP, FA and DE algorithms.

The rest of the paper is organized as follows. Section 2 gives a review of background and related work. The passive target localization system based on the noisy TOA measurements is presented in Sect. 3. In Sect. 4, the ML objective function is derived. The SDP method for solving the passive target localization problem is presented in Sect. 5. Section 6 introduces the DE algorithm, followed by the corresponding improvements. FA with an adaptive attractiveness function is described in Sect. 7. Section 8 introduces an improved AHFADE algorithm. In Sect. 9, the CRLB for passive target localization problem is derived. Numerical simulation results are provided in Sect. 10. The conclusions and some possible directions for future work are given in Sect. 11.

2 Background and related work

The accuracy of passive target position has always been an important and challenging issue in many applications that has received significant interest among the research community (Shen et al. 2012). It is well known that the reliability and accuracy of the localization depend on the geometric configuration of the transmitter, receivers and target, the measurement accuracy and the environment (e.g., ambient noise) (Bishop et al. 2010). Consequently, numerous localization algorithms have been proposed in the literature for different applications, which can be divided into two categories: range-based and range-free algorithms (Chowdhury et al. 2016). The range-based localization algorithms utilize range measurements, such as distance or angle information between the unknown position of the target and the known position of each receiver in order to estimate the position of the target. These algorithms use various measurement techniques, such as TOA (Shen et al. 2012), time difference of arrival (TDOA) (Huang et al. 2015), received signal strength (RSS) (Li et al. 2017), angle of arrival (AOA) (Xu and Doğançay 2015) or combination of them (Coluccia and Fascista 2018). The localization accuracy is dependent on the distance or angle measurements to estimate the position of the target for a given

localization problem. Generally, the unknown position of the target can be determined using geometric methods such as triangulation, trilateration and multilateration or by applying an estimation method (Asmaa et al. 2014). Among them, the TOA is a promising method for target localization based on a set of receivers with known positions, which has attracted considerable research focus, due to its low cost and high localization accuracy (Sadowski and Spachos 2018). Conversely, the range-free localization algorithms do not require range or angle information between sensor nodes, and they utilize only connectivity information for localization. Basically, wireless sensor networks (WSNs) have tremendous ability to collect and transfer information of the deployed sensors, which can be used to determine the possible position of the target in their radio range (Halder and Ghosal 2016). The well-known range-free localization algorithms are: the centroid or weighted centroid algorithm, distance vector hop (DV-hop) and approximate point-in-triangulation test (APIT) (Singh and Sharma 2015). Compared with range-based algorithms, the range-free algorithms do not need additional hardware to determine the actual range; hence, they are cost-effective, easy to implement and have a low power consumption; however, this leads to less accurate localization performance (Halder and Ghosal 2016).

One of the most commonly used estimation methods to estimate the unknown position of the target is the nonlinear least squares (NLS) estimator (Zekavat and Buehrer 2011). Hence, the estimated target position can be obtained by minimizing the squared sum of the measurement errors with respect to the unknown target position. Thus, the given localization problem can be formulated as nonlinear minimization problem, which does not have closed-form solution, and it is difficult to solve.

Local search optimization algorithms have been widely applied for solving various localization problems (Kaur et al. 2016). These optimization algorithms can be classified into gradient-based and direct search methods, which only perform local search around the initial solution (Rao and Rao 2009). Different gradient-based algorithms such as steepest decent, Gauss–Newton and conjugate gradient have been proposed in the literature to find the unknown position of the target for the given NLS problem (Arora 2004). However, local search algorithms require feasible starting point to find the global optimum (Rao and Rao 2009). Therefore, these algorithms cannot guarantee convergence to the global optimum of a multimodal optimization problem and thus, cannot be used to solve passive target localization problem. In order to obtain a closed-form solution, the nonlinear optimization problem has been linearized using linear least squares (LLS) and weighed least squares (WLS) algorithms under the small Gaussian noise assumption (Wang 2015; Einemo and So 2015). To further improve the localization performance, especially in the presence of high-noise mea-

surements, the constrained weighted least squares (CWLS) algorithm is developed, to obtain the estimated position of the target (Qu and Xie 2016). The CWLS rearranges the nonlinear equations into a set of linear equations, by explicitly incorporating the relationship between the target position and the auxiliary variable as a second-order equality constraint. In fact, the CWLS problem can be formulated as a quadratically constrained quadratic program (QCQP), which is converted to an unconstrained optimization problem. In this regard, the simulation results have shown that the RMSE of the CWLS algorithm can achieve the CRLB accuracy under small measurement errors (Lin et al. 2013). Another widely employed estimation method in the literature is the ML estimator, which maximizes the likelihood function of the unknown target position (Destino and Abreu 2011). However, the corresponding ML objective function is a highly nonlinear and non-convex function, where conventional optimization methods are not suitable for solving this kind of optimization problem. In order to overcome the non-convexity of the ML estimation problem, it can be transformed into a convex optimization problem using SDP or second-order cone programming (SOCP) (Kocuk et al. 2016). In this respect, both the SDP and SOCP methods can be effectively employed to approximately solve non-convex optimization problems, and find a global or near-global optimal solution. Simulation results have shown that the SDP method provides better localization accuracy compared to SOCP method. However, these methods cannot provide a high estimation accuracy in the presence of significant measurement noise (Biswas et al. 2006). To overcome this problem, there has been great interest to improve and develop efficient metaheuristic optimization algorithms, which can successfully find the global optimal solution for a given localization problem, without using gradient information during the search process.

Numerous metaheuristic algorithms like PSO, CSA, artificial bee colony (ABC), etc., have been widely applied in order to solve the localization problem in terms of determining the unknown position of the target (Kulkarni et al. 2019; Jiang et al. 2018). Therefore, there is still a need to choose an appropriate optimization algorithm as the straightforward way to minimize the localization error in all environments for a given localization problem. In this regard, the PSO algorithm and its improved variants have been employed to improve the localization accuracy for the passive target localization problem based on TDOA measurements (Cakir et al. 2014). The considered localization algorithm estimates the target position based on the nonlinear least squares residuals. The comparative analysis has shown that the improved variants of PSO algorithm can provide higher localization accuracy in comparison with the conventional PSO and well-known LLS and WLS algorithms for the given problem. Furthermore, the TDOA passive localization algorithm based on the ML objective function and CSA has been proposed to esti-

mate the possible position of the target (Jiang et al. 2018). In the proposed algorithm, the Lévy flight mechanism has been adopted to effectively avoid being trapped in local optimum of a multimodal objective function by improving population diversity. Additionally, the simulation results show that the CSA has more efficient global exploration ability of the search space than existing conventional PSO algorithm. The DE algorithm and its hybrid variants such as PSO and DE (PSODE) (Zhang et al. 2015a) and DE and FA (HFDLA) (Harikrishnan et al. 2016) have been also proposed to estimate unknown position of the target in order to improve the localization performance and overcome the drawbacks of getting trapped in a local minimum during the evolution process.

Therefore, this paper proposes an improved robust AHFADE algorithm, based on the hybridization of DE and FA, to solve the multimodal passive target localization problem with high accuracy even in highly noisy environments.

3 Localization problem

In this section, the passive target localization problem based on TOA measurements is presented to estimate the unknown position of the target in LOS environment. The proposed localization system consists of N receivers, $\{R_i\}_{i=1}^N$, whose known positions are $\mathbf{x}_i^r = [x_i^r \ y_i^r]^T \in \mathbb{R}^2, \forall i \in \{1, 2, \dots, N\}$ such that $N \geq 3$, where T_x is the transmitter located at the origin of the coordinate system, i.e., $\mathbf{x}_T = [0 \ 0]^T \in \mathbb{R}^2$, as illustrated in Fig. 1. Assume that the true coordinates of the target are $\mathbf{x} = [x \ y]^T \in \mathbb{R}^2$.

The passive target localization problem uses noisy TOA measurements, where the transmitter emits a signal and the receivers subsequently receive the signal reflected from the target. Thus, each receiver captures two signals in a row: one direct signal from the transmitter and the reflected signal from the target. It is assumed that the transmitter and receivers are perfectly synchronized, and the target reflects the TOA signal in all directions without any interaction with the transmitter and receivers in the network (Shen et al. 2012). The additive white Gaussian noise is widely used in localization algorithms, which is a reasonable assumption in LOS conditions (Wu et al. 2016). In order to find the estimated position of the target, there must be at least three TOA measurements. In fact, the noisy TOA measurements are composed of time from the transmitter to the unknown target position, and the time from the target to each receiver, which are functions of the unknown target position, i.e.,

$$t_i = \frac{1}{c} (\|\mathbf{x}\|_2 + \|\mathbf{x} - \mathbf{x}_i^r\|_2) + \bar{n}_i, \quad \forall i \in \{1, 2, \dots, N\}, \quad (1)$$

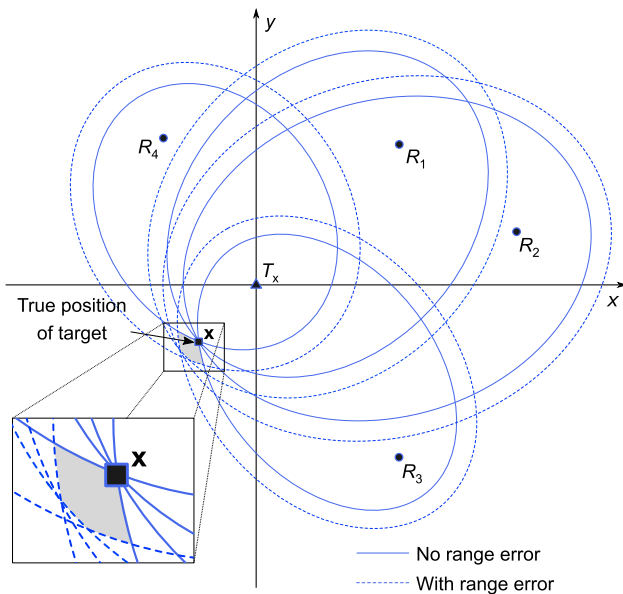


Fig. 1 Passive target localization system using noisy TOA measurements

where $\|\cdot\|_2$ denotes the Euclidean distance in two-dimensional space, c is the speed of light, and \tilde{n}_i is the zero-mean Gaussian measurement noise with variance of σ_i^2 . Then, multiplying both sides of Eq. (1) by the speed of light c , yields range measurements (transmitter–target–receiver distances) denoted by $\{\tilde{d}_i\}_{i=1}^N$, which can be expressed as follows:

$$\begin{aligned} \tilde{d}_i &= c \cdot t_i \\ &= d_i + n_i, \quad \forall i \in \{1, 2, \dots, N\}, \end{aligned} \tag{2}$$

where the true range measurement $d_i = \|\mathbf{x}\|_2 + \|\mathbf{x} - \mathbf{x}_i^r\|_2$ is the sum of transmitter–target and target–receiver distances, $n_i = c\tilde{n}_i$ follows Gaussian distribution $\mathcal{N}(0, \sigma_{ni}^2)$ with zero-mean and variance of $\sigma_{ni}^2 = c^2\sigma_i^2$. Hence, the TOA range measurements for every transmitter and receiver ($T_x - R_i$) pair have positive errors, which imply that the range measurements are greater than the true ones, as shown in Fig. 1, (Zhang et al. 2014).

In the absence of measurement errors, from the geometric interpretation, the sum of transmitter–target and target–receiver ranges d_i at time t_i , defines the solid-line ellipse E_i , whose foci are placed at transmitter and receiver positions \mathbf{x}_T and \mathbf{x}_i^r , respectively, as shown in Fig. 1. Therefore, the true range d_i of each transmitter and receiver ($T_x - R_i$) pair is constant for every point on an ellipse E_i , which can be defined as follows:

$$E_i = \left\{ (x, y) \in \mathbb{R}^2 : d_i = \sqrt{x^2 + y^2} + \sqrt{(x - x_i^r)^2 + (y - y_i^r)^2} \right\}. \tag{3}$$

Hence, the vector of true range measurements can be expressed as follows:

$$\mathbf{d}(\mathbf{x}) = \begin{bmatrix} \|\mathbf{x}\|_2 + \|\mathbf{x} - \mathbf{x}_1^r\|_2 \\ \|\mathbf{x}\|_2 + \|\mathbf{x} - \mathbf{x}_2^r\|_2 \\ \vdots \\ \|\mathbf{x}\|_2 + \|\mathbf{x} - \mathbf{x}_N^r\|_2 \end{bmatrix}. \tag{4}$$

Therefore, $\mathbf{d}(\mathbf{x})$ defines a set of ellipses $\{E_i\}_{i=1}^N$, with respect to different transmitter and receiver pairs $T_x - R_i$, $\forall i \in \{1, 2, \dots, N\}$, with two foci placed at positions \mathbf{x}_T and \mathbf{x}_i^r , respectively. Thus, the true position of the passive target \mathbf{x} is obtained by the intersection of three or more solid line ellipses $\{E_i\}_{i=1}^{N \geq 3}$, as shown in Fig. 1. Therefore, the target position is obtained as the unique solution in the absence of measurement errors.

Additionally, in the presence of measurement errors, the vector form of Eq. (2) can be expressed as follows:

$$\tilde{\mathbf{d}} = \mathbf{d}(\mathbf{x}) + \mathbf{n}, \tag{5}$$

where $\mathbf{n} = [n_1 \ n_2 \ \dots \ n_N]^T$ is the vector of zero-mean noise. In this case, three or more dashed-line ellipses derived from noisy TOA measurements do not have a unique intersection point. Thus, the estimated position of the target can be found within the shaded region caused by error in the TOA measurements, as depicted in Fig. 1. Consequently, the localization accuracy is related to the size of this region which includes the target, i.e., the obtained small region can result in high localization accuracy.

Hence, in this paper, the main goal is to estimate the actual position of the target based on noisy TOA measurements by solving a highly nonlinear and multimodal ML estimation problem, as explained in the next section.

4 Maximum likelihood method

The estimation of the unknown position of the passive target can be obtained through maximizing the likelihood function. Under the assumptions of Gaussian noisy TOA measurements, which are independent and identically distributed, with a single transmitter, it is possible to express the likelihood function $L(\mathbf{x})$ for the target position (Shen et al. 2012) as follows:

$$\begin{aligned} L(\mathbf{x}) = f(\tilde{\mathbf{d}}|\mathbf{x}) &= \frac{1}{(2\pi)^{N/2} \det(\mathbf{C})^{1/2}} \\ &\times \exp\left(-\frac{1}{2}(\tilde{\mathbf{d}} - \mathbf{d}(\mathbf{x}))^T \mathbf{C}^{-1}(\tilde{\mathbf{d}} - \mathbf{d}(\mathbf{x}))\right), \end{aligned} \tag{6}$$

where $f(\tilde{\mathbf{d}}|\mathbf{x})$ denotes the probability density function of the measurements, $\det(\cdot)$ is the determinant of matrix, and \mathbf{C} is the diagonal covariance matrix given as:

$$\mathbf{C} = \text{diag}\{\sigma_{n1}^2, \dots, \sigma_{nN}^2\}. \tag{7}$$

The logarithm of the likelihood function is used more often in practice as it turns the product of the terms into summation. Thus, the logarithm of Eq. (6) can be expressed as:

$$\ln L(\mathbf{x}) = k - \frac{1}{2}(\tilde{\mathbf{d}} - \mathbf{d}(\mathbf{x}))^T \mathbf{C}^{-1}(\tilde{\mathbf{d}} - \mathbf{d}(\mathbf{x})), \tag{8}$$

where $k = \ln(1/((2\pi)^{N/2} \det(\mathbf{C})^{1/2}))$ is a constant independent of \mathbf{x} .

Consequently, the ML estimator requires the maximization of the log-likelihood function, which is equivalent to minimizing the negative logarithm of the likelihood function. Hence, the ML estimation problem can be formulated as:

$$\min_{\mathbf{x} \in \mathbb{R}^2} J_{\text{ML}}(\mathbf{x}), \tag{9}$$

where the corresponding ML objective function $J_{\text{ML}}(\mathbf{x})$ can be written as:

$$J_{\text{ML}}(\mathbf{x}) = (\tilde{\mathbf{d}} - \mathbf{d}(\mathbf{x}))^T \mathbf{C}^{-1}(\tilde{\mathbf{d}} - \mathbf{d}(\mathbf{x})). \tag{10}$$

Therefore, the estimated target position $\hat{\mathbf{x}}$ can be obtained by minimizing the objective function $J_{\text{ML}}(\mathbf{x})$ with respect to \mathbf{x} , as follows:

$$\hat{\mathbf{x}} = \arg \min_{\mathbf{x} \in \mathbb{R}^2} (J_{\text{ML}}(\mathbf{x})). \tag{11}$$

Figure 2 shows the corresponding contour plot for a given optimization problem and the gradient vectors, which indicate the direction of minimum of the objective function $J_{\text{ML}}(\mathbf{x})$.

From the contour plot in Fig. 2, it can be noticed that the objective function $J_{\text{ML}}(\mathbf{x})$ is a highly nonlinear and non-convex function, whose global minimum $\hat{\mathbf{x}}$ corresponds to the unknown position of the target. In respect of this, the global optimal solution of the ML estimation problem cannot be obtained in closed form. Thus, in order to solve this kind of complex optimization problem, it is necessary to use sophisticated optimization algorithms, which are described in the next sections.

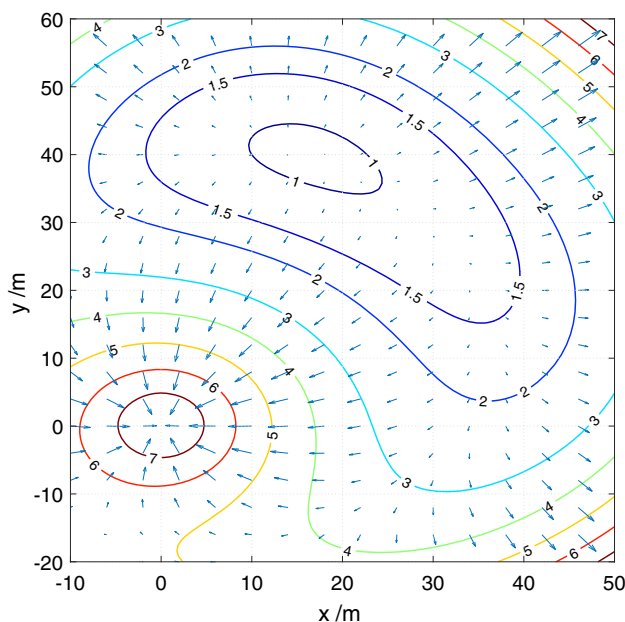


Fig. 2 Illustration of the objective function $J_{\text{ML}}(\mathbf{x})$ with the corresponding contour plot

5 Semidefinite programming method

In this section, the SDP method is applied to transform the non-convex ML estimation problem into a convex optimization problem. According to Eqs. (9) - (11), the ML estimation problem with respect to \mathbf{x} can be formulated as:

$$\hat{\mathbf{x}} = \arg \min_{\mathbf{x} \in \mathbb{R}^2} (\tilde{\mathbf{d}} - \mathbf{d}(\mathbf{x}))^T \mathbf{C}^{-1}(\tilde{\mathbf{d}} - \mathbf{d}(\mathbf{x})). \tag{12}$$

Based on the approach (Wang and Wu 2016), the vector $\mathbf{d}(\mathbf{x})$ can be introduced as follows:

$$\mathbf{d}(\mathbf{x}) = \mathbf{H}\mathbf{g}, \tag{13}$$

in which the $(N + 1) \times 1$ vector \mathbf{g} is defined as:

$$\mathbf{g} = [\|\mathbf{x}\|_2 \ \|\mathbf{x} - \mathbf{x}_1^r\|_2 \ \|\mathbf{x} - \mathbf{x}_2^r\|_2 \ \dots \ \|\mathbf{x} - \mathbf{x}_N^r\|_2]^T, \tag{14}$$

and

$$\mathbf{H} = [\mathbf{1}_N \ \mathbf{I}_N] = \begin{bmatrix} 1 & 1 & \dots & 0 & 0 \\ 1 & 0 & \dots & 0 & 0 \\ \vdots & \vdots & \ddots & \vdots & \vdots \\ 1 & 0 & \dots & 0 & 1 \end{bmatrix}. \tag{15}$$

here $\mathbf{1}_N$ and \mathbf{I}_N are column vector of length N with all entries equal to one and the $N \times N$ identity matrix, respectively. The equality constraints are introduced between the transmitter \mathbf{x}_T and the unknown position of the target \mathbf{x} , and that target

and i th receiver located at \mathbf{x}_i^r , denoted by $[\mathbf{g}]_{1,1}^2 = \|\mathbf{x}\|_2^2$ and $[\mathbf{g}]_{i,i}^2 = \|\mathbf{x} - \mathbf{x}_i^r\|_2^2, \forall i \in \{1, 2, \dots, N\}$, respectively. Then, the optimization problem in Eq. (12) can be rewritten as the following constrained optimization problem:

$$\begin{aligned} \min_{\mathbf{x}, \mathbf{g}} \quad & (\tilde{\mathbf{d}} - \mathbf{H}\mathbf{g})^T \mathbf{C}^{-1} (\tilde{\mathbf{d}} - \mathbf{H}\mathbf{g}) \\ \text{s.t.} \quad & [\mathbf{g}]_{1,1}^2 = \|\mathbf{x}\|_2^2, \\ & [\mathbf{g}]_{i,i}^2 = \|\mathbf{x} - \mathbf{x}_i^r\|_2^2, \\ & \forall i \in \{1, 2, \dots, N\}. \end{aligned} \tag{16}$$

The objective function for the above optimization problem, by corresponding algebraic manipulation, can be expressed as follows:

$$\begin{aligned} & (\tilde{\mathbf{d}} - \mathbf{H}\mathbf{g})^T \mathbf{C}^{-1} (\tilde{\mathbf{d}} - \mathbf{H}\mathbf{g}) \\ &= \begin{bmatrix} \mathbf{g} \\ 1 \end{bmatrix}^T \begin{bmatrix} \mathbf{H}^T \mathbf{C}^{-1} \mathbf{H} & -\mathbf{H}^T \mathbf{C}^{-1} \tilde{\mathbf{d}} \\ -\tilde{\mathbf{d}}^T \mathbf{C}^{-1} \mathbf{H} & \tilde{\mathbf{d}}^T \mathbf{C}^{-1} \tilde{\mathbf{d}} \end{bmatrix} \begin{bmatrix} \mathbf{g} \\ 1 \end{bmatrix}. \end{aligned} \tag{17}$$

Based on the matrix property $\mathbf{x}^T \mathbf{A} \mathbf{x} = \text{Tr}(\mathbf{x} \mathbf{x}^T \mathbf{A})$ and introducing the matrix notation $\mathbf{G} = \mathbf{g} \mathbf{g}^T$, then Eq. (17) is given as follows:

$$\begin{aligned} & \begin{bmatrix} \mathbf{H}^T \mathbf{C}^{-1} \mathbf{H} & -\mathbf{H}^T \mathbf{C}^{-1} \tilde{\mathbf{d}} \\ -\tilde{\mathbf{d}}^T \mathbf{C}^{-1} \mathbf{H} & \tilde{\mathbf{d}}^T \mathbf{C}^{-1} \tilde{\mathbf{d}} \end{bmatrix} \begin{bmatrix} \mathbf{g} \\ 1 \end{bmatrix} \\ &= \text{Tr} \left(\begin{bmatrix} \mathbf{g} \\ 1 \end{bmatrix} \begin{bmatrix} \mathbf{g}^T & 1 \end{bmatrix} \mathbf{P} \right) = \text{Tr} \left(\begin{bmatrix} \mathbf{G} & \mathbf{g} \\ \mathbf{g}^T & 1 \end{bmatrix} \mathbf{P} \right), \end{aligned} \tag{18}$$

in which

$$\mathbf{P} = \begin{bmatrix} \mathbf{H}^T \mathbf{C}^{-1} \mathbf{H} & -\mathbf{H}^T \mathbf{C}^{-1} \tilde{\mathbf{d}} \\ -\tilde{\mathbf{d}}^T \mathbf{C}^{-1} \mathbf{H} & \tilde{\mathbf{d}}^T \mathbf{C}^{-1} \tilde{\mathbf{d}} \end{bmatrix}, \tag{19}$$

where $\text{Tr}(\cdot)$ denote the trace of a square matrix.

Introducing the $z = \mathbf{x}^T \mathbf{x}$, the constraints can be expressed as:

$$\begin{aligned} [\mathbf{G}]_{1,1} &= \|\mathbf{x}\|_2^2 = z, \\ [\mathbf{G}]_{i,i} &= \|\mathbf{x} - \mathbf{x}_i^r\|_2^2 = \mathbf{x}^T \mathbf{x} - 2\mathbf{x}^T \mathbf{x}_{i-1}^r + (\mathbf{x}_{i-1}^r)^T \mathbf{x}_{i-1}^r \\ &= z - 2\mathbf{x}^T \mathbf{x}_{i-1}^r + (\mathbf{x}_{i-1}^r)^T \mathbf{x}_{i-1}^r, \\ &\forall i \in \{2, \dots, N + 1\}. \end{aligned} \tag{20}$$

Then, according to Eqs. (18) and (20), the optimization problem in Eq. (16) can be reformulated as:

$$\begin{aligned} \min_{\mathbf{x}, \mathbf{g}, \mathbf{G}, z} \quad & \text{Tr} \left(\begin{bmatrix} \mathbf{G} & \mathbf{g} \\ \mathbf{g}^T & 1 \end{bmatrix} \mathbf{P} \right) \\ \text{s.t.} \quad & [\mathbf{G}]_{1,1} = z, \\ & [\mathbf{G}]_{i,i} = z - 2\mathbf{x}^T \mathbf{x}_{i-1}^r + (\mathbf{x}_{i-1}^r)^T \mathbf{x}_{i-1}^r, \end{aligned}$$

$$\begin{aligned} & \forall i \in \{2, \dots, N + 1\}, \\ & \mathbf{G} = \mathbf{g} \mathbf{g}^T, \\ & z = \mathbf{x}^T \mathbf{x}. \end{aligned} \tag{21}$$

Furthermore, the Cauchy–Schwartz inequality for the off-diagonal elements of the matrix \mathbf{G} can be written as:

$$\begin{aligned} [\mathbf{G}]_{i,j} &= \|\mathbf{x} - \mathbf{x}_{i-1}^r\|_2 \|\mathbf{x} - \mathbf{x}_{j-1}^r\|_2 \\ &\geq \left| (\mathbf{x} - \mathbf{x}_{i-1}^r)^T (\mathbf{x} - \mathbf{x}_{j-1}^r) \right| \\ &= \left| \mathbf{x}^T \mathbf{x} - (\mathbf{x}_{i-1}^r + \mathbf{x}_{j-1}^r)^T \mathbf{x} + (\mathbf{x}_{i-1}^r)^T \mathbf{x}_{j-1}^r \right|, \\ &\forall i, j \in \{1, 2, \dots, N + 1\}, \quad i \neq j, \end{aligned} \tag{22}$$

with $\mathbf{x}_0^r = \mathbf{x}_T = [0 \ 0]^T$.

Due to the nonlinear equality constraints $\mathbf{G} = \mathbf{g} \mathbf{g}^T$ and $z = \mathbf{x}^T \mathbf{x}$, the optimization problem in Eq. (21) is a non-convex, where the global optimal solution is very difficult to obtain. Therefore, the non-convex equality constraints $\mathbf{G} = \mathbf{g} \mathbf{g}^T$ and $z = \mathbf{x}^T \mathbf{x}$, can be relaxed into the convex inequality constraints, as follows:

$$\begin{aligned} \mathbf{G} - \mathbf{g} \mathbf{g}^T &\succeq \mathbf{0}, \\ z - \mathbf{x} \mathbf{x}^T &\succeq \mathbf{0}. \end{aligned} \tag{23}$$

After applying the Schur complement (Boyd and Vandenberghe 2004), these constraints can be equivalently expressed as:

$$\begin{aligned} \begin{bmatrix} \mathbf{G} & \mathbf{g} \\ \mathbf{g}^T & 1 \end{bmatrix} &\succeq \mathbf{0}, \\ \begin{bmatrix} z & \mathbf{x} \\ \mathbf{x}^T & \mathbf{I}_2 \end{bmatrix} &\succeq \mathbf{0}. \end{aligned} \tag{24}$$

It should be noted that the matrices given in Eq. (24) are symmetric and positive semidefinite matrices, and therefore, the inequality constraints in Eq. (24) should be convex functions.

Finally, based on the above relaxation, the optimization problem in Eq. (21) becomes a convex problem, which can be written as follows:

$$\begin{aligned} \min_{\mathbf{x}, \mathbf{g}, \mathbf{G}, z} \quad & \text{Tr} \left(\begin{bmatrix} \mathbf{G} & \mathbf{g} \\ \mathbf{g}^T & 1 \end{bmatrix} \mathbf{P} \right) \\ \text{s.t.} \quad & [\mathbf{G}]_{1,1} = z, \\ & [\mathbf{G}]_{i,i} = z - 2\mathbf{x}^T \mathbf{x}_{i-1}^r + (\mathbf{x}_{i-1}^r)^T \mathbf{x}_{i-1}^r, \\ & \forall i \in \{2, \dots, N + 1\}, \\ & [\mathbf{G}]_{i,j} \geq \left| z - (\mathbf{x}_{i-1}^r + \mathbf{x}_{j-1}^r)^T \mathbf{x} + (\mathbf{x}_{i-1}^r)^T \mathbf{x}_{j-1}^r \right|, \\ & \forall i, j \in \{1, 2, \dots, N + 1\}, \quad i \neq j, \end{aligned}$$

$$\begin{aligned} \begin{bmatrix} \mathbf{G} & \mathbf{g} \\ \mathbf{g}^T & 1 \end{bmatrix} &\succeq \mathbf{0}, \\ \begin{bmatrix} z & \mathbf{x} \\ \mathbf{x}^T & \mathbf{I}_2 \end{bmatrix} &\succeq \mathbf{0}. \end{aligned} \tag{25}$$

Therefore, the SDP problem given in Eq. (25) is a convex one, which can be efficiently implemented and solved by the CVX toolbox (Grant and Boyd 2014) using SeDuMi as the solver (Grant and Boyd 2008).

6 Differential evolution algorithm and the proposed improved versions

In this section, the conventional DE algorithm is first introduced. Then, a brief description of the improved adaptive versions of the DE such as SHADE and JADE algorithms with the mutation operator DE/current-to-pbest/1 is presented and implemented in this work.

6.1 Conventional DE algorithm

The DE is a population-based algorithm, which is based on four phases: initialization, mutation, crossover and selection, which are briefly summarized as follows.

6.1.1 Initialization

Generally, the population of NP random individuals at the current generation G , where each individual is expressed by n -dimensional vector as a potential solution, can be represented as follows:

$$\begin{aligned} \left\{ \mathbf{x}_i^{(G)} : x_{i,j}^{(G)} \in \left[x_{i,j}^L, x_{i,j}^U \right] \right\}, \\ \forall i \in \{1, 2, \dots, NP\}, \forall j \in \{1, 2, \dots, n\} \end{aligned} \tag{26}$$

where $x_{i,j}^L$ and $x_{i,j}^U$ denote the lower and upper bounds of the j th component of the i th individual $x_{i,j}$, respectively. Therefore, the initial j th component of the i th individual is randomly generated according to a uniform distribution within the corresponding boundary constraints $x_{i,j}^L \leq x_{i,j}^{(0)} \leq x_{i,j}^U$, which can be defined as follows:

$$x_{i,j}^{(0)} = x_{i,j}^L + \text{rand}_j \left(x_{i,j}^U - x_{i,j}^L \right), \tag{27}$$

where rand_j is a uniformly distributed random number in the range $[0, 1]$.

6.1.2 Mutation

The mutation operator plays a vital role during the evolution process, where a mutant vector for each target vector $\mathbf{x}_i^{(G)}$ can be expressed as follows:

$$\mathbf{v}_i^{(G+1)} = \left[v_{i,1}^{(G+1)} \ v_{i,2}^{(G+1)} \ \dots \ v_{i,j}^{(G+1)} \ \dots \ v_{i,n}^{(G+1)} \right]^T. \tag{28}$$

In recent years, a number of different mutation operators for exploration of the search space, have been developed and proposed in the literature (Mohamed and Suganthan 2018), which are described as follows: DE/rand/1

$$\mathbf{v}_i^{(G+1)} = \mathbf{x}_{r_1}^{(G)} + F \left(\mathbf{x}_{r_2}^{(G)} - \mathbf{x}_{r_3}^{(G)} \right), \tag{29}$$

DE/best/1

$$\mathbf{v}_i^{(G+1)} = \mathbf{x}_{\text{best}}^{(G)} + F \left(\mathbf{x}_{r_1}^{(G)} - \mathbf{x}_{r_2}^{(G)} \right), \tag{30}$$

DE/current-to-best/1

$$\mathbf{v}_i^{(G+1)} = \mathbf{x}_i^{(G)} + F \left(\mathbf{x}_{\text{best}}^{(G)} - \mathbf{x}_i^{(G)} \right) + F \left(\mathbf{x}_{r_1}^{(G)} - \mathbf{x}_{r_2}^{(G)} \right), \tag{31}$$

where r_1, r_2 and r_3 are distinct integers randomly generated from the set $\{1, 2, \dots, NP\} \setminus \{i\}$, the $\mathbf{x}_{\text{best}}^{(G)}$ denotes the individual with the best objective function value and $F \in [0, 1]$ is the scale factor.

6.1.3 Crossover

After the mutation phase, the evolution process involves the crossover operator to generate a new vector, which is called the trial vector, in order to increase the diversity of the population. The DE algorithm uses the binomial crossover operator, which combines the components of the target vector $\mathbf{x}_i^{(G)}$ and the corresponding mutant vector $\mathbf{v}_i^{(G+1)}$ to generate the trial vector $\mathbf{u}_i^{(G+1)}$ according to

$$u_{i,j}^{(G+1)} = \begin{cases} v_{i,j}^{(G+1)} & \text{if } \text{rand}_{i,j} \leq \text{CR} \vee j = j_{\text{rand}} \\ x_{i,j}^{(G)} & \text{otherwise} \end{cases} \tag{32}$$

where the crossover rate $\text{CR} \in [0, 1]$ is a pre-defined rate, and j_{rand} is an integer randomly generated from set $\{1, 2, \dots, n\}$. Thus, if and only if $\text{rand}_{i,j} \leq \text{CR}$ or $j = j_{\text{rand}}$, then the binomial crossover operator copies the j th variable of mutant vector $\mathbf{v}_i^{(G+1)}$ to its corresponding element in the trial vector $\mathbf{u}_i^{(G+1)}$. Otherwise, the parameter is inherited from the corresponding target vector $\mathbf{x}_i^{(G)}$.

6.1.4 Selection

The next phase is selection, in which the DE compares the objective function value of the trial vector $f \left(\mathbf{u}_i^{(G+1)} \right)$, with corresponding objective function value of the target vector $f \left(\mathbf{x}_i^{(G)} \right)$. If and only if the objective function value of the trial vector $f \left(\mathbf{u}_i^{(G+1)} \right)$ is less than or equal to the objective

function value of the target vector $f(\mathbf{x}_i^{(G)})$, then $\mathbf{u}_i^{(G+1)}$ is set to $\mathbf{x}_i^{(G+1)}$. Otherwise, the old target vector $\mathbf{x}_i^{(G)}$ is retained. Therefore, the selection operator can be defined as follows:

$$\mathbf{x}_i^{(G+1)} = \begin{cases} \mathbf{u}_i^{(G+1)} & \text{if } f(\mathbf{u}_i^{(G+1)}) \leq f(\mathbf{x}_i^{(G)}) \\ \mathbf{x}_i^{(G)} & \text{otherwise} \end{cases}, \quad (33)$$

where $\mathbf{x}_i^{(G+1)}$ is the target vector selected for the next generation.

The algorithm is repeated until the termination criterion (the maximum number of generations G_{max}) is satisfied.

6.2 Improved DE algorithm

In this paper, the powerful efficient DE variants named JADE and SHADE have been proposed with the aim to provide the dynamically adapted control parameters for each individual in each generation of evolution according to Cauchy distribution for $F_i^{(G)}$ and normal distribution for $CR_i^{(G)}$ (Zhang and Sanderson 2009; Tanabe and Fukunaga 2013). Therefore, the control parameters $F_i^{(G)}$ and $CR_i^{(G)}$ for each individual $\mathbf{x}_i^{(G)}$ in each generation of evolution are independently generated, as follows:

$$F_i^{(G)} = randc_i(\mu_F^{(G)}, 0.1), \quad (34)$$

$$CR_i^{(G)} = randn_i(\mu_{CR}^{(G)}, 0.1), \quad (35)$$

where $randc_i(\mu_F^{(G)}, 0.1)$ is a random variable distributed according to the Cauchy distribution with median $\mu_F^{(G)}$ and scale parameter 0.1, and $randn_i(\mu_{CR}^{(G)}, 0.1)$ represents a random number generated from normal distribution with mean $\mu_{CR}^{(G)}$ and standard deviation 0.1.

The parameters $\mu_F^{(0)}$ and $\mu_{CR}^{(0)}$ are initialized to 0.5. If $F_i^{(G)} > 1$, then $F_i^{(G)}$ is set to 1, while when $F_i^{(G)} < 0$, $F_i^{(G)}$ can be regenerated using Eq. (34). Similarly, if $CR_i^{(G)} > 1$, then $CR_i^{(G)}$ is truncated to 1; otherwise if $CR_i^{(G)}$ is less than 0, then $CR_i^{(G)}$ is set to 0.

In each generation, all successful values of $F_i^{(G)}$ and $CR_i^{(G)}$ are saved in the sets S_F and S_{CR} , respectively. Hence, at the end of each generation, the parameters $\mu_F^{(G)}$ and $\mu_{CR}^{(G)}$ can be updated as below:

$$\mu_F^{(G+1)} = \begin{cases} (1-c)\mu_F^{(G)} + c \cdot \text{mean}_{WL}(S_F) & \text{if } S_F \neq \emptyset \\ (1-c)\mu_F^{(G)} + c \cdot \text{rand}(0, 1) & \text{otherwise} \end{cases}, \quad (36)$$

$$\mu_{CR}^{(G+1)} = \begin{cases} (1-c)\mu_{CR}^{(G)} + c \cdot \text{mean}_{WA}(S_{CR}) & \text{if } S_{CR} \neq \emptyset \\ (1-c)\mu_{CR}^{(G)} + c \cdot \text{rand}(0, 1) & \text{otherwise} \end{cases}, \quad (37)$$

where c is the learning rate, which is set to $c = 0.1$ (Zhang and Sanderson 2009). Here, the $\text{mean}_{WL}(\cdot)$ and $\text{mean}_{WA}(\cdot)$ denote the weighted Lehmer mean and weighted arithmetic mean, respectively, which can be expressed as follows:

$$\text{mean}_{WL}(S_F) = \frac{\sum_{k=1}^L w_k \cdot S_{F,k}^2}{\sum_{k=1}^L w_k \cdot S_{F,k}}, \quad (38)$$

$$\text{mean}_{WA}(S_{CR}) = \frac{\sum_{k=1}^L w_k \cdot S_{CR,k}^2}{\sum_{k=1}^L w_k \cdot S_{CR,k}}, \quad (39)$$

in which $L = |S_F| = |S_{CR}|$ denotes the size of the sets S_F and S_{CR} , respectively. Then, the weight w_k can be calculated as follows:

$$w_k = \frac{\Delta f_i}{\sum_{k=1}^L \Delta f_i}, \quad (40)$$

where $\Delta f_i = |f(\mathbf{u}_i^{(G)}) - f(\mathbf{x}_i^{(G)})|$ denotes the absolute difference between the objective function values of trial vector and target vector.

6.3 The DE/current-to-pbest/1 mutation operator

One of the improved DE variants, named JADE, introduces the effective mutation operator DE/current-to-pbest/1 that accelerates the convergence speed of the algorithm toward the global optimal solution (Zhang and Sanderson 2009). In this regard, the DE/current-to-pbest/1 is used in this work due to its simplicity of implementation, in order to provide more effective search direction during the evolution process. Then, the corresponding mutation vector based on the proposed DE/current-to-pbest/1 mutation operator can be generated, as follows:

$$\mathbf{v}_i^{(G)} = \mathbf{x}_i^{(G)} + F_i^{(G)}(\mathbf{x}_{pbest}^{(G)} - \mathbf{x}_i^{(G)}) + F_i^{(G)}(\mathbf{x}_{r1}^{(G)} - \mathbf{x}_{r2}^{(G)}), \quad (41)$$

where $F_i^{(G)}$ is the scale factor for each individual generated from the Cauchy distribution according to Eq. (34) and $\mathbf{x}_{pbest}^{(G)}$ is randomly selected from the top ($p \times 100\% \times NP$) individuals in the current population with $p \in (0, 1]$.

Obviously, from Eq. (41), it can be observed that the mutation vector exploits the nearby region of each $\mathbf{x}_i^{(G)}$, in the direction of the solution $\mathbf{x}_{pbest}^{(G)}$, which further improves the search ability of the algorithm, especially in the later stage of evolution process. Consequently, the global optimal solution can be easily reached for the given optimization problem.

7 Firefly algorithm and the proposed improved version

7.1 Firefly algorithm

The FA is one of the most powerful swarm-based metaheuristic algorithms used for solving multimodal optimization problems, which has been developed by Xin-She Yang (Yang 2010b). In essence, the FA is based on the following three assumptions:

- All fireflies are unisex.
- Attractiveness is proportional to their brightness, implying that the less bright firefly will move to the brighter firefly. The firefly will continue to move randomly if no brighter firefly is found in a swarm.
- The brightness of a firefly represents the objective function value for a given optimization problem. Thus, for a minimization problem, the brightness of each firefly is inversely proportional to the value of the objective function.

The first step in the application of the FA is to randomly generate an initial swarm of NP fireflies over the n -dimensional search space. Generally, in order to properly create the FA, there are two important issues that need to be defined, such as the variation of light intensity and the formulation of attractiveness between fireflies in the swarm.

The light intensity $I(r)$ varies with distance, which can be described as the following monotonically decreasing exponential function of the distance

$$I(r) = I_0 e^{-\gamma r^2}, \tag{42}$$

where I_0 is the original light intensity and γ is a fixed light absorption coefficient. The parameter γ has a crucial impact on the convergence speed of the algorithm. Theoretically, the parameter γ should take any value from the interval $\gamma \in [0, \infty)$. In most applications, it typically varies from 0.1 to 10, and could be usually set to 1.

The attractiveness function $\beta(r_{i,j})$ between two fireflies i and j is proportional to the light intensity $I(r)$, and can be defined as follows:

$$\beta(r_{i,j}) = \beta_0 e^{-\gamma r_{i,j}^2}, \tag{43}$$

where $\beta_0 \in [0, 1]$ is the maximum attractiveness at $r_{i,j} = 0$, i.e., when two fireflies are found at the same point of search space.

The Euclidean distance $r_{i,j}$, between any pair of fireflies i and j at positions \mathbf{x}_i and \mathbf{x}_j , respectively, can be obtained as follows:

$$r_{i,j} = \|\mathbf{x}_i - \mathbf{x}_j\|_2 = \sqrt{\sum_{k=1}^n (x_{i,k} - x_{j,k})^2}. \tag{44}$$

Here, $x_{i,k}$ and $x_{j,k}$ are the k th element of the i th and j th firefly positions within the search space, respectively.

The search process of FA depends on the attraction between fireflies in the swarm. In this regard, the movement of the less bright firefly i toward another brighter firefly j determines the new position $\mathbf{x}_i^{(G+1)}$ at $(G + 1)$ th iteration, which can be generated as follows:

$$\mathbf{x}_i^{(G+1)} = \mathbf{x}_i^{(G)} + \beta(r_{i,j}) (\mathbf{x}_j^{(G)} - \mathbf{x}_i^{(G)}) + \alpha \mathbf{e}_i^{(G)}. \tag{45}$$

Hence, Eq. (45) consists of three terms. The first term gives the current position of the i th firefly, the second term is related to the attraction, while the third term represents the random motion of i th firefly. According to Eq. (45), the randomization parameter α is normally selected within range $[0, 1]$, where the $\mathbf{e}_i^{(G)}$ is a vector of random numbers defined by the Gaussian distribution, i.e., $\mathbf{e}_i^{(G)} = (rand_{i,j} - 0.5)$, and $rand_{i,j}$ is a random number uniformly distributed in $[0, 1]$.

7.2 Improved version of firefly algorithm

The conventional FA suffers from the problem of being trapped in local optimum of a multimodal objective function, which can lead to premature convergence. In this regard, to solve the highly nonlinear and multimodal optimization problems, there is a need to modify the FA (Yang 2009; Wang et al. 2017).

According to Eq. (43), it is obvious that at the early stage of the evolution process, the distance between fireflies and the global optimal solution is extremely large; thus, the attractiveness tends to be zero and becomes nearly non-existent. Then, the movement of fireflies is based on the random walk through the search space, so the convergence of the algorithm is not guaranteed. On the other hand, with the increase in generations, the distance between fireflies and the global optimal solution is extremely small; thus, the attractiveness remains constant. Therefore, the modification in the search process of the FA is still needed, in order to enhance the optimization performance in aspect of balance between the global exploration and local exploitation abilities.

In order to provide an appropriate balance between exploration and exploitation of the search space of the conventional FA, this paper proposed the improved attractiveness function $\tilde{\beta}(r_{i,j})$, which can be created, as follows:

$$\tilde{\beta}(r_{i,j}) = \beta_0 e^{-\gamma r_{i,j}^2 \frac{G}{G_{\max}}} \frac{f_{\text{best}}}{f_{\text{mean}}}, \tag{46}$$

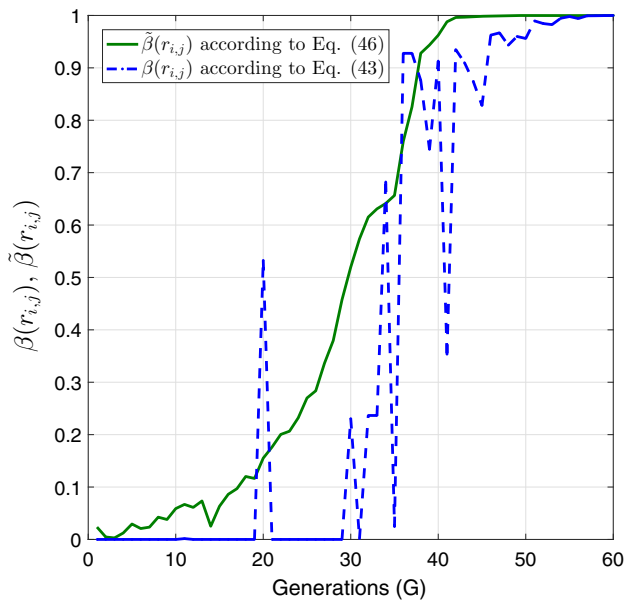


Fig. 3 Comparison between the attractiveness functions $\beta(r_{i,j})$ and $\tilde{\beta}(r_{i,j})$ during the evolution process

where f_{mean} and f_{best} are the mean and best values of the objective function in the previous generation, respectively.

Based on Eq. (46), the updated firefly position can be rewritten as:

$$\mathbf{x}_i^{(G+1)} = \mathbf{x}_i^{(G)} + \tilde{\beta}(r_{i,j}) \left(\mathbf{x}_j^{(G)} - \mathbf{x}_i^{(G)} \right) + \alpha \mathbf{e}_i^{(G)}. \quad (47)$$

Simulation results obtained for attractiveness functions $\beta(r_{i,j})$ and $\tilde{\beta}(r_{i,j})$ according to Eq. (43) (dashed line) and Eq. (46) (solid line), respectively, during the evolution process are presented in Fig. 3.

As presented in Fig. 3, in the early stage of the evolution process, the attractiveness function $\beta(r_{i,j})$ defined in Eq. (43) tends to be zero, then, it oscillates between 0 and 1.0, which can slow down the search process, and therefore, the convergence of the algorithm is not guaranteed.

On the contrary, the proposed attractiveness $\tilde{\beta}(r_{i,j})$ defined in Eq. (46) gradually increases with growth of generations, in order to enhance the ability of finding the global optimal solution, as shown in Fig. 3. This modification helps to maintain the diversity within the swarm and improves the convergence speed of the algorithm in order to create balance between the global exploration and local exploitation ability of the proposed algorithm.

Therefore, in the evolution process, the improved attractiveness $\tilde{\beta}(r_{i,j})$ is adaptively increased and significantly outperforms the original attractiveness $\beta(r_{i,j})$ in search ability.

8 Adaptive hybrid firefly differential evolution algorithm

Based on the above considerations, this section introduces the AHFADE algorithm, based on the hybridization of the DE with the FA. The main goal of the proposed algorithm is to create an efficient search strategy by incorporating mutation operators of the DE into the FA, to achieve the global optimal solution with high accuracy and fast convergence. The mutation operator DE/rand/1 has strong global exploration with slow convergence speed, while the DE/current-to-pbest/1, which has been proposed in JADE (Zhang and Sanderson 2009), has more suitable local exploitation ability that leads to faster convergence speed. Therefore, in order to enhance the diversity and convergence of the FA, and to prevent the algorithm from falling into local optimum of a multimodal objective function, the following two modifications are proposed.

The first modification is performed to improve the exploration of FA using the mutation operator DE/rand/1 by replacing the term $\alpha \mathbf{e}_i$ in Eq. (47) with $F_i^{(G)} \left(\mathbf{x}_{r_2}^{(G)} - \mathbf{x}_{r_3}^{(G)} \right)$. For implementing the first modification, the $F_i^{(G)}$ from Eq. (34) is substituted in Eq. (47) and $\mathbf{x}_j^{(G)}$ in Eq. (47) is replaced with $\mathbf{x}_{r_1}^{(G)}$ from Eq. (29). Then, the expression for updating the new position of the i th firefly is given as follows:

$$\begin{aligned} \mathbf{x}_i^{(G+1)} = & \mathbf{x}_i^{(G)} + \tilde{\beta}(r_{i,j}) \left(\mathbf{x}_{r_1}^{(G)} - \mathbf{x}_i^{(G)} \right) \\ & + F_i^{(G)} \left(\mathbf{x}_{r_2}^{(G)} - \mathbf{x}_{r_3}^{(G)} \right). \end{aligned} \quad (48)$$

After mathematical transformations, Eq. (48) can be rewritten as follows:

$$\begin{aligned} \mathbf{x}_i^{(G+1)} = & \left(1 - \tilde{\beta}(r_{i,r_1}) \right) \mathbf{x}_i^{(G)} + \tilde{\beta}(r_{i,r_1}) \mathbf{x}_{r_1}^{(G)} \\ & + F_i^{(G)} \left(\mathbf{x}_{r_2}^{(G)} - \mathbf{x}_{r_3}^{(G)} \right), \end{aligned} \quad (49)$$

where r_{i,r_1} is the distance between fireflies i and r_1 at the positions $\mathbf{x}_i^{(G)}$ and $\mathbf{x}_{r_1}^{(G)}$, respectively.

The second modification is aimed to improve the exploitation of the FA using the mutation operator DE/current-to-pbest/1. To achieve this, the third term in Eq. (49) is replaced with $F_i^{(G)} \left(\mathbf{x}_{r_1}^{(G)} - \mathbf{x}_{r_2}^{(G)} \right)$ and $\mathbf{x}_{r_1}^{(G)}$ is substituted with $\left(\mathbf{x}_{\text{pbest}}^{(G)} - \mathbf{x}_i^{(G)} \right)$, which is given in Eq. (41). As a result, the new expression for updating the new position of the i th firefly can be expressed as:

$$\begin{aligned} \mathbf{x}_i^{(G+1)} = & \left(1 - \tilde{\beta}(r_{i,\text{pbest}}) \right) \mathbf{x}_i^{(G)} + \tilde{\beta}(r_{i,\text{pbest}}) \left(\mathbf{x}_{\text{pbest}}^{(G)} - \mathbf{x}_i^{(G)} \right) \\ & + F_i^{(G)} \left(\mathbf{x}_{r_1}^{(G)} - \mathbf{x}_{r_2}^{(G)} \right), \end{aligned} \quad (50)$$

where $r_{i, pbest}$ is the distance between fireflies i and $pbest$ at the positions $\mathbf{x}_i^{(G)}$ and $\mathbf{x}_{pbest}^{(G)}$, respectively.

Based on the above considerations, an adaptive parameter is proposed in this work that relies on the normalized objective function values to automatically switch between global exploration and local exploitation, which can be expressed as:

$$\Delta = 1 - \left| \frac{f_{\text{mean}} - f_{\text{best}}}{f_{\text{worst}} - f_{\text{best}}} \right|, \tag{51}$$

where f_{mean} , f_{best} and f_{worst} are the mean, best and worst objective function values of individuals in the previous generation, respectively.

Obviously, the balance between global exploration and local exploitation can be controlled by changing the value of Δ . Therefore, according to Eq. (51), when the value of Δ is close to 0, the population diversity is low, which corresponds to global exploration of the search space. Hence, Eq. (49) can be applied in order to explore the search space and locate the region of the global optimum. On the other hand, when the value of Δ is close to 1, the population diversity is high, which corresponds to local exploitation of the search space. In this process, Eq. (50) can be employed to improve the local search ability and enhance convergence speed. Therefore, in the evolution process, the new position of i th firefly can be updated based on adaptive parameter Δ , as shown below:

$$\mathbf{v}_i^{(G+1)} = \begin{cases} (1 - \tilde{\beta}(r_{i,r_1})) \mathbf{x}_i^{(G)} + \tilde{\beta}(r_{i,r_1}) \mathbf{x}_{r_1}^{(G)} \\ + F_i^{(G)} (\mathbf{x}_{r_2}^{(G)} - \mathbf{x}_{r_3}^{(G)}), & \Delta \leq \omega \\ (1 - \tilde{\beta}(r_{i,pbest})) \mathbf{x}_i^{(G)} + \tilde{\beta}(r_{i,pbest}) (\mathbf{x}_{pbest}^{(G)} - \mathbf{x}_i^{(G)}) \\ + F_i^{(G)} (\mathbf{x}_{r_1}^{(G)} - \mathbf{x}_{r_2}^{(G)}), & \text{otherwise} \end{cases} \tag{52}$$

where $\omega = 0.5$ is the predefined threshold value.

These modifications have significant influence on the convergence speed and population diversity of the proposed algorithm. In this manner, the exploration and exploitation abilities of the proposed algorithm are strengthened. Additionally, the crossover and selection operators are the same as in the conventional DE algorithm and can be easily implemented into the structure of the proposed AHFADE algorithm.

The flowchart of the proposed AHFADE algorithm for the passive target localization problem is illustrated in Fig.4.

The methodology of the proposed AHFADE algorithm, described above, can be divided into following steps:

Step 1 Initialize parameters

Initialize parameters of the proposed AHFADE algorithm, including the population size, the maximum number of generations, the lower and upper bounds.

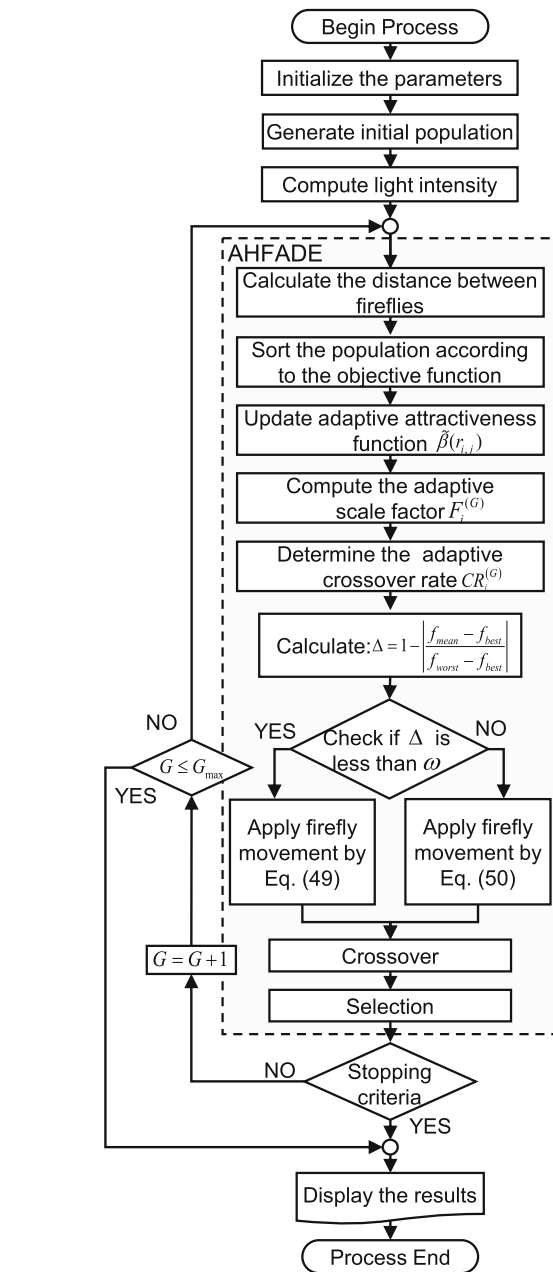


Fig. 4 The flowchart of the proposed AHFADE algorithm

Step 2 Generate the initial population of fireflies

The position of fireflies in the swarm is initialized uniformly and randomly in the n -dimensional search space.

Step 3 Compute light intensity

Compute light intensity of each firefly in current generation.

Step 4 The following process is repeated until the stopping criterion is reached

- Step 5 *Calculate the distance between fireflies*
Determine the distance r_{ij} between any two fireflies \mathbf{x}_i and \mathbf{x}_j in the swarm, according to Eq. (44).
- Step 6 *Sort the population*
The fireflies are sorted according to objective function values.
- Step 7 *Update the proposed attractiveness $\tilde{\beta}(r_{i,j})$*
The proposed attractiveness $\tilde{\beta}(r_{i,j})$ is updated according to the normalized objective function values, as defined in Eq. (46).
- Step 8 *Compute the adaptive scale factor $F_i^{(G)}$*
Using Eq. (34) update the value of adaptive scale factor $F_i^{(G)}$.
- Step 9 *Determine the adaptive crossover rate $CR_i^{(G)}$*
Compute the adaptive crossover rate $CR_i^{(G)}$ according to Eq. (35).
- Step 10 *Calculate the value of the adaptive parameter Δ*
Calculate the value of the adaptive parameter Δ using Eq. (51).
- Step 11 *Check parameter Δ and move the fireflies*
If $\Delta \leq \omega$, then Eq. (49) is applied; otherwise, when $\Delta > \omega$, Eq. (50) is used.
- Step 12 *Crossover operator*
The crossover operator is applied to the population according to Eq. (32).
- Step 13 *Selection operator*
The selection operator defined in Eq. (33) is applied.
- Step 14 *Stopping criterion*
Stop the AHFADE algorithm if a termination criterion is satisfied and continue to Step 15; otherwise, go to Step 4 and repeat the search for the global optimal solution.
- Step 15 *Display of the results*
Display the best solution found and its corresponding objective function value.

Finally, the AHFADE algorithm can be implemented for solving the passive localization problem. Consequently, Fig. 5 shows the position of fireflies during evolution process with 60 fireflies in the generation.

Based on the initially created swarm, the proposed algorithm guides the swarm of fireflies in each generation toward better solution, as shown in Fig. 5. It is clearly seen that at the end of the evolution process, the swarm of fireflies will gather around the global optimal solution in the search space, and as a result, the estimated position of the target is found, which is shown in the same figure. In this way, the proposed AHFADE algorithm uses 60 generations to satisfy the stopping condition and obtain the global optimal solution of the considered ML objective function.

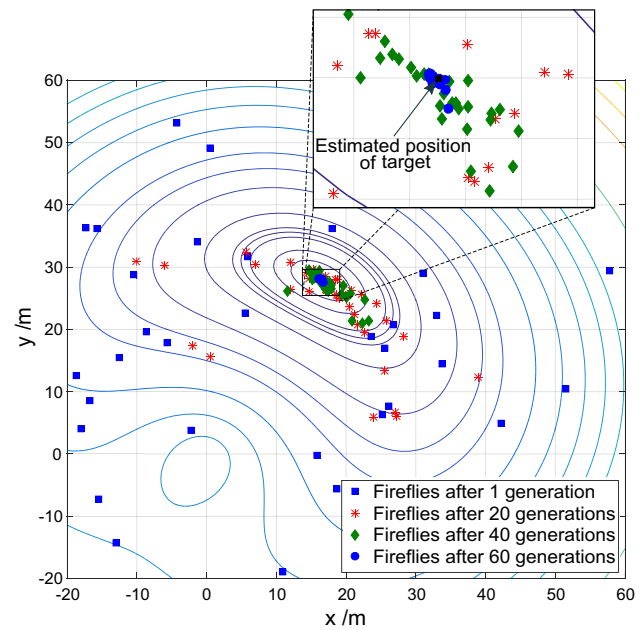


Fig. 5 The position of fireflies during the evolution process

9 Cramér–Rao lower bound

In the passive target localization problem, the CRLB establishes a lower bound on the covariance matrix and provides a useful tool for evaluating the performance of any unbiased estimator (Shen et al. 2012). The CRLB is obtained from the diagonal elements of the inverse of the Fisher information matrix (FIM), denoted by $\mathbf{I}(\mathbf{x})$. Based on the probability density function $f(\tilde{\mathbf{d}}|\mathbf{x})$ given in Eq. (6), the FIM of the proposed target localization system is given as follows:

$$\begin{aligned} \mathbf{I}(\mathbf{x}) &= E \left[\left(\frac{\partial \ln(f(\tilde{\mathbf{d}}|\mathbf{x}))}{\partial \mathbf{x}} \right) \left(\frac{\partial \ln(f(\tilde{\mathbf{d}}|\mathbf{x}))}{\partial \mathbf{x}} \right)^T \right] \\ &= -E \left[\frac{\partial^2 \ln(f(\tilde{\mathbf{d}}|\mathbf{x}))}{\partial \mathbf{x} \partial \mathbf{x}^T} \right]. \end{aligned} \quad (53)$$

Then, the FIM can be written as:

$$\mathbf{I}(\mathbf{x}) = \begin{bmatrix} I_{xx} & I_{xy} \\ I_{yx} & I_{yy} \end{bmatrix}, \quad (54)$$

where the corresponding elements are defined as follows:

$$\begin{aligned} I_{xx} &= \sum_{i=1}^N \frac{1}{\sigma_{ni}^2} \left(\frac{x - x_i^r}{\|\mathbf{x} - \mathbf{x}_i^r\|_2} + \frac{x}{\|\mathbf{x}\|_2} \right)^2, \\ I_{xy} &= I_{yx} = \sum_{i=1}^N \frac{1}{\sigma_{ni}^2} \left(\frac{x - x_i^r}{\|\mathbf{x} - \mathbf{x}_i^r\|_2} + \frac{x}{\|\mathbf{x}\|_2} \right) \end{aligned} \quad (55)$$

$$\times \left(\frac{y - y_i^r}{\|\mathbf{x} - \mathbf{x}_i^r\|_2} + \frac{y}{\|\mathbf{x}\|_2} \right), \tag{56}$$

$$I_{yy} = \sum_{i=1}^N \frac{1}{\sigma_{ni}^2} \left(\frac{y - y_i^r}{\|\mathbf{x} - \mathbf{x}_i^r\|_2} + \frac{y}{\|\mathbf{x}\|_2} \right)^2. \tag{57}$$

Therefore, the inverse of the FIM is expressed as follows:

$$\mathbf{I}^{-1} = \frac{1}{\det(\mathbf{I})} \begin{bmatrix} I_{yy} & -I_{xy} \\ -I_{yx} & I_{xx} \end{bmatrix}. \tag{58}$$

Derivations of Eqs. (55)–(57) are given in Appendix A. The CRLB of passive target location vector components is given by the r th diagonal element of the inverse of the FIM, as follows:

$$\text{CRLB}([\mathbf{x}]_r) = \left[\mathbf{I}^{-1} \right]_{r,r}, \tag{59}$$

where $[\mathbf{I}^{-1}]_{r,r}$ is the r th row and the r th column element of the corresponding matrix \mathbf{I}^{-1} and $r = 1, 2$. Hence, the CRLB on the variance of an unbiased estimator $\hat{\mathbf{x}}$ is expressed as:

$$E \left[(\hat{\mathbf{x}} - \mathbf{x}) (\hat{\mathbf{x}} - \mathbf{x})^T \right] \geq \text{Tr} \left(\mathbf{I}^{-1}(\mathbf{x}) \right), \tag{60}$$

where $\hat{\mathbf{x}}$ is the estimated value of \mathbf{x} .

10 Experimental study

In this section, experiments are conducted to evaluate the localization performance and to perform the statistical comparison of the AHFADE algorithm with other well-known algorithms on CEC2014 benchmark problems. In this regard, the obtained numerical results are outlined into two subsections, which are described below.

10.1 Statistical comparisons of the proposed AHFADE algorithm on CEC2014 benchmark

In this section, experiments are carried out to compare the proposed AHFADE with well-known state-of-the-art algorithms, such as SHADE (Tanabe and Fukunaga 2013), jDE (Brest et al. 2006), FA (Yang 2010b) and Lévy-flight FA (LFA) (Yang 2010a) algorithms on CEC2014 benchmark. The formulation of test functions and optimization problems used in this analysis has been described in (Liang et al. 2013). The CEC2014 benchmark considers the single objective real-parameter numerical optimization and consists of 30 test functions, where the dimensions of the search space are $D = 10, 30, 50$ and 100 . Based on the characteristics of the objective functions defined in CEC2014 benchmark

problem, the 30 test functions can be categorized into the following groups:

- $f_1 - f_3$ represent optimization problems with unimodal objective functions,
- $f_4 - f_{16}$ denote simple multimodal objective functions,
- $f_{17} - f_{22}$ are hybrid functions, where the variables are divided into subcomponents, in which each component is defined using a different basic function,
- $f_{23} - f_{30}$ denote composition functions, which combine the properties of the sub-functions while maintaining the continuity in the region of the global optimum.

In order to perform statistical analysis and compare the performance of the proposed AHFADE algorithm, the solution error measure $(f(\hat{\mathbf{x}}) - f(\mathbf{x}^*))$ has been employed, where $\hat{\mathbf{x}}$ denotes the best solution of the algorithm obtained in one run and \mathbf{x}^* represents the well-known global optimal solution of the corresponding CEC 2014 test function. Experiments for each algorithm on each test function have been independently run for 50 times, and statistical results are provided. According to the recommendations, the termination criteria are set to $10000D$ (Liang et al. 2013), and the population size is set to $N_p = 100$ (Tanabe and Fukunaga 2013). For all considered problems, the search space is bounded by $[-100, 100]^D$. To perform evaluation, from a statistical point of view, the obtained solutions have been analyzed and compared using two nonparametric statistical hypothesis tests, e.g., Wilcoxon signed-rank test and Friedman test.

Firstly, the Wilcoxon signed-rank test has been employed to determine whether the first algorithm obtained statistically better solution compared to the second algorithm. In the analysis, the Wilcoxon signed-rank test has been applied with significance level $\alpha = 0.05$. Therefore, in the results, the R^+ denotes the sum of ranks where the first algorithm outperformed the second, and R^- represents the sum of ranks for which the first algorithm performed worse than the second algorithm. Furthermore, in the corresponding columns designated with signs $+, \approx, -$ (better, equal and worse), we have denoted the number of test functions where the first algorithm is better than, equal to, or worse than the second algorithm, respectively. Based on (Derrac et al. 2011), for the null hypothesis of the Wilcoxon signed-rank test, it is assumed that "there is no difference between the mean results of the two samples". On the other hand, the alternative hypothesis states that "there is a difference in the mean results of the two samples". Therefore, p value has been employed in the statistical analysis and compared to the significance level α . Thus, the null hypothesis can be rejected, when the p value is less than or equal to the $\alpha = 0.05$. The compared results have been indicated with the following three signs $(+, -, \approx)$ according to the results of the statistical test. In

this regard, the plus (+) sign designates that the first algorithm is significantly better than the second, minus (−) sign means that the first algorithm is significantly worse than the second, and approximation (\approx) sign denotes that there is no significant difference between two algorithms.

Secondly, the Friedman test has been employed to obtain the ranks of all algorithms over every test function on all considered dimensions D of the search space, in order to find the significant differences between the performance of two or more algorithms. In this respect, the algorithm with the lowest rank denotes the best performing algorithm, while the algorithm which has the highest rank is considered as the worst. According to (Derrac et al. 2011), for the null hypothesis of the Friedman test, it is assumed that "there is no difference among the performance of all algorithms", whereas the alternative hypothesis states that "there is a difference among the performance of all algorithms".

The computational results of the proposed AHFADE and other considered algorithms on CEC2014 benchmark problems are presented in Table 1, where "Mean" represents the mean value of the objective function of the best individual, "STD" represents the standard deviation, and "Sign" denotes whether the considered algorithm has better (+), similar (\approx) or worse (−) performance compared to the proposed AHFADE algorithm. From the numerical results in Table 1, it can be observed that the proposed AHFADE algorithm obtains the best "Mean" and "STD" values on most test functions compared to other considered algorithms. However, on hybrid functions f_{17} and f_{21} , and composite function f_{28} the AHFADE algorithm has the similar performance to jDE algorithm over the dimensions $D = 30, 50$ and 100 . Compared to the jDE and SHADE algorithms, the AHFADE algorithm achieves the similar performance on functions f_{19} and f_4 on dimensions $D = 50$ and $D = 30$, respectively, as well as on composite functions f_{26} and f_{28} on $D = 50$. Furthermore, the AHFADE algorithm has worse performance than jDE and SHADE algorithms on unimodal function f_2 , multimodal function f_7 and composite functions f_{23} and f_{24} on dimensions of the problem $D = 30, 50$ and 100 , respectively. In comparison with the FA and LFA algorithms, it can be observed that AHFADE significantly outperforms these algorithms on all considered dimensions. However, on multimodal problems f_5 , f_{12} and f_{16} over the dimensions $D = 50$ and 100 , the proposed algorithm achieves worse performance compared to the FA and LFA algorithms. Therefore, it can be concluded that the proposed AHFADE algorithm has clearly the best performance among the SHADE, FA and LFA algorithms, and for higher dimensions of the problem, e.g., $D = 30, 50$ and 100 , it achieves similar performance to jDE algorithm, especially on composite functions. In this way, the proposed algorithm successfully finds promising solutions on all problems and all dimensions.

In order to perform the statistical comparison of the performance of considered algorithms, the results have been analyzed using Wilcoxon signed-rank test. In this regard, in Table 2 the statistical results of applying Wilcoxon's signed-rank test between AHFADE and jDE, SHADE, FA and LFA algorithms using CEC2014 test functions on over all dimensions have been shown.

From the results in Table 2, it can be observed that for the dimensions $D = 10$ and $D = 30$, the proposed AHFADE algorithm is significantly better than SHADE, FA and LFA algorithms. However, the proposed AHFADE algorithm has higher R^+ values than R^- when compared to the jDE algorithm on the dimensions $D = 10$ and $D = 30$. On the other hand, for the dimensions $D = 50$ and $D = 100$ the proposed algorithm achieves better performance than FA and LFA algorithms. Additionally, compared to the jDE and SHADE algorithms it is observed that for $D = 50$ and $D = 100$ the AHFADE algorithm provides higher R^+ values than R^- . Therefore, from the results, it can be concluded that the proposed AHFADE algorithm can achieve better performance compared to the individual performances of SHADE and FA algorithms. This shows the effectiveness of the proposed hybridization between DE and FA algorithms which is achieved by introducing the dynamically adapted parameter into the mutation operator, and incorporating the crossover and selection operators of DE algorithm into the FA.

Furthermore, to compare the overall performance of multiple algorithms, the Friedman test has been applied. In this regard, the Table 3 presents the average ranks according to Friedman test, for the proposed AHFADE and other considered algorithms on different CEC2014 benchmark functions for $D = 10, 30, 50$ and 100 dimensions. In this table, the algorithm with the best rank is shown in bold and second best is underlined.

From the results of the statistical analysis using the Friedman test, given in Table 3, it can be concluded that the proposed AHFADE algorithm achieves the best performance and has the lowest rank among all considered algorithms. Furthermore, it can be observed that the p values computed through Friedman test for all considered test functions in all dimensions are less than significance level $\alpha = 0.05$. Therefore, based on the hypothesis, it can be concluded that there is a significant difference between the performances of the considered algorithms. According to the statistical analysis, it can be concluded that the proposed AHFADE algorithm has an effective mutation strategy and improved adaptive techniques for setting the control parameter values. Furthermore, the obtained results also show that the hybridization between DE and FA algorithms significantly enhances the performance of the AHFADE algorithm, which demonstrates the effectiveness of the modifications proposed in this paper.

Table 1 Experimental results on 30 CEC2014 test functions in terms of mean and standard deviation of function value

<i>f</i>	<i>D</i>	AHFADE Mean (STD) Sign	SHADE	jDE	FA	LFA
<i>f</i> ₁	10	3.78E+02(3.42E+02)	2.08E+06(1.43E+06)+	2.96E+03(1.04E+04)+	3.04E+08(1.68E+08)+	4.54E+07(1.92E+07)+
	30	6.99E+06(4.48E+06)	1.5E+08(5.6E+07)+	1.52E+08(5.45E+07)+	3.2E+09(9.7E+08)+	1.6E+09(3.3E+08)+
	50	3.6E+07(1.68E+07)	2.41E+08(6.02E+07)+	2.12E+08(5.99E+07)+	8.5E+09(1.9E+09)+	5.7E+09(9.3E+08)+
	100	3.18E+08(8E+07)	8.96E+08(1.97E+08)+	8.56E+08(1.68E+08)+	2.1E+10(3.5E+09)+	1.7E+10(1.8E+09)+
<i>f</i> ₂	10	1.83E-03(8.53E-03)	2.66E+05(1.69E+05)+	2.48E+02(3.17E+02)+	1.23E+10(3.42E+09)+	7.52E+09(1.82E+09)+
	30	2.12E+08(1.3E+08)	2.8E+07(8.81E+06)-	1.22E-02(3.91E-02)-	1.13E+11(1.9E+10)+	1.2E+11(1.3E+10)+
	50	4.1E+09(2E+09)	2.67E+08(7.63E+07)-	2.45E+03(3.68E+03)-	2.8E+11(2.9E+10)+	2.6E+11(1.9E+10)+
	100	3.75E+10(7.6E+09)	5.33E+09(1.01E+09)-	1E+07(9E+07)-	6.4E+11(4.5E+10)+	6.1E+11(3.7E+10)+
<i>f</i> ₃	10	3.86E-04(2.75E-03)	1.16E+03(5.93E+02)+	4.76E-03(1.3E-02)+	1.71E+05(5.47E+05)+	2.23E+04(4.28E+03)+
	30	1.5E+03(6.6E+02)	2.39E+04(6.5E+03)+	2.45E+04(6.72E+03)+	8.8E+05(2.6E+06)+	1.54E+05(2.05E+04)+
	50	1.07E+04(2.15E+03)	3.37E+05(2.7E+05)+	2.96E+05(2.1E+05)+	8.1E+05(2.06E+06)+	2.87E+05(2.98E+04)+
	100	4.13E+04(6.3E+03)	7.42E+05(3.36E+05)+	7.05E+05(3.05E+05)+	1.01E+06(7.6E+05)+	7.18E+05(4.07E+04)+
<i>f</i> ₄	10	2.88E+01(1.29E+01)	3.24E+01(8.02)+	1.53E+01(1.69E+01)-	2.34E+03(1.12E+03)+	9.19E+02(3.25E+02)+
	30	1.67E+02(3.14E+01)	1.59E+02(2.16E+01)≈	1.6E+02(2.2E+01)≈	3.56E+04(9.02E+03)+	2.79E+04(3.88E+03)+
	50	6.56E+02(1.92E+02)	2.71E+02(4.33E+01)-	1.76E+02(3.88E+01)-	1.1E+05(2.26E+04)+	9.25E+04(1.19E+04)+
	100	3.99E+03(1.06E+03)	1.08E+03(1.33E+02)-	5.53E+02(1.11E+02)-	2.88E+05(3.86E+04)+	2.59E+05(2.86E+04)+
<i>f</i> ₅	10	1.76E+01(6.51)	2.09E+01(1.56E-01)+	1.97E+01(2.82)+	2.03E+01(7.42E-02)+	2.03E+01(6.52E-02)+
	30	2.1E+01(3.84E-01)	2.13E+01(7.8E-02)+	2.19E+01(2.87E-02)+	2.09E+01(4.95E-02)≈	2.02E+01(4.28E-02)≈
	50	2.13E+01(1.33E-01)	2.14E+01(5.78E-02)≈	2.1E+01(6.5E-02)-	2.11E+01(3.33E-02)-	2.11E+01(3.59E-02)-
	100	2.15E+01(3.78E-02)	2.15E+01(3.24E-02)≈	2.12E+01(3.5E-02)-	2.13E+01(2.01E-02)-	2.13E+01(2.27E-02)-
<i>f</i> ₆	10	6.42E-01(6.92E-01)	6.53(1.39)+	6.66E-01(1.04)≈	1.31E+01(9.04E-01)+	9.83(4.4E-01)+
	30	8.6(7.66)	3.89E+01(3.6)+	1.05E+01(2.46)+	4.8E+01(1.4)+	4.19E+01(7.14E-01)+
	50	4.19E+01(2.29E+01)	6.82E+01(4.79)+	6.74E+01(4.65)+	8.37E+01(1.97)+	7.58E+01(1.12)+
	100	1.48E+02(2.48E+01)	1.55E+02(7.34)≈	1.67E+02(7.96)+	1.76E+02(2.66)+	1.65E+02(1.71)+
<i>f</i> ₇	10	1.13E-02(1.23E-02)	9.19E-01(9.43E-02)+	9.68E-02(4.62E-02)+	1.91E+02(4.81E+01)+	1.29E+02(2.69E+01)+
	30	1.17(2.91E-01)	1.21(6.9E-02)+	1.15E-02(1.6E-02)-	1.19E+03(1.52E+02)+	1.05E+03(9.86E+01)+
	50	2.25E+01(1.52E+01)	3.49(6.4E-01)-	7.2E-03(1E-02)-	2.63E+03(3.17E+02)+	2.54E+03(1.66E+02)+
	100	3.01E+02(8.06E+01)	5.34E+01(9.76)-	5.5E-03(1.2E-02)-	5.82E+03(2.94E+02)+	5.7E+03(2.87E+02)+

Table 1 continued

f	D	AHFADE Mean (STD) Sign	SHADE	jDE	FA	LFA
f_8	10	1.833(1.71)	3.84E+01(7.52)+	3.9E-02(1.95E-01)-	1.19E+02(1.35E+01)+	7.38E+01(7.47)+
	30	8.4(5.6)	2.2E+02(2.15E+01)+	1.34E+01(3.55)+	4.99E+02(2.65E+01)+	4.36E+02(1.67E+01)+
	50	2.05E+01(9.7)	4.3E+02(3.1E+01)+	3.6E+01(8.51)+	9.24E+02(4.31E+01)+	8.62E+02(2.31E+01)+
	100	9.23E+01(4.31E+01)	1.02E+03(3.77E+01)+	1.36E+03(2.16E+01)+	2.03E+03(5.9E+01)+	1.96E+03(3.94E+01)+
	10	2.282(1.411)	5.81E+01(1.24E+01)+	4.23(2.02)+	1.17E+02(1.5E+01)+	7.56E+01(8.8)+
f_9	30	2.11E+02(4.72E+01)	2.72E+02(2.93E+01)+	2.95E+02(3.24E+01)+	6E+02(4.81E+01)+	5.26E+02(2.81E+01)+
	50	4.41E+02(4.65E+01)	5.07E+02(3.24E+01)+	4.89E+02(3.01E+01)+	1.17E+03(6.61E+01)+	1.08E+03(4.67E+01)+
	100	1.11E+03(5.6E+01)	1.14E+03(4.87E+01)+	1.21E+03(4.99E+01)+	2.48E+03(1.19E+02)+	2.38E+03(7.09E+01)+
	10	6.66E-01(1.39)	1.58E+03(3.09E+02)+	8.1E+01(8.34E+01)+	2.05E+03(9.97E+01)+	1.25E+03(1.05E+02)+
	30	1.52E+01(4.54E+01)	7.33E+03(5.37E+02)+	5.03E+02(2.07E+02)+	8.59E+03(2.32E+02)+	7.26E+03(2.72E+02)+
f_{10}	50	1.51E+03(1.37E+03)	1.42E+04(7.38E+02)+	1.51E+03(1.73E+02)-	1.55E+04(2.87E+02)+	1.39E+04(3.41E+02)+
	100	6.87E+03(2.78E+03)	3.17E+04(1.28E+03)+	3.98E+03(6.76E+02)-	3.38E+04(3.96E+02)+	3.18E+04(4.46E+02)+
	10	8.74E+02(4.18E+02)	2.15E+03(2.61E+02)+	1.34E+02(1.21E+02)-	2.04E+03(1.39E+02)+	1.43E+03(1.31E+02)+
	30	8.14E+03(5.19E+02)	8.9E+03(6E+02)+	8.78E+03(5.71E+02)+	8.49E+03(1.88E+02)+	7.37E+03(2.35E+02)-
	50	1.55E+04(7.54E+02)	1.61E+04(5.28E+02)+	5.74E+03(1E+03)-	1.54E+04(2.68E+02)≈	1.39E+04(3.07E+02)-
f_{11}	100	3.45E+04(8.54E+02)	3.44E+04(8.72E+03)≈	1.58E+04(4.72E+03)-	3.35E+04(4.71E+02)-	3.15E+04(4.24E+02)-
	10	1.7E-02(1.55E-02)	3.5(9.59E-01)+	9.54E-02(7.31E-02)+	1.06(1.86E-01)+	9.63E-01(1.33E-01)+
	30	4.33E-01(8.66E-01)	5.82(9.76E-01)+	1.19(6.32E-01)+	2.5(2.52E-01)+	2.51(2.34E-01)+
	50	5.01(2.2)	6.79(9.22E-01)+	6.45(9.03E-01)+	3.6(2.35E-01)-	3.42(2.79E-01)-
	100	6.43(1.26)	6.78(5.6E-01)≈	6.86(5.91E-01)+	4.26(1.99E-01)-	4.2(2.08E-01)-
f_{12}	10	1.6E-01(1.4E-01)	5.82E-01(1.34E-01)+	1E-01(3.91E-02)-	4.95(9.15E-01)+	3.89(4.39E-01)+
	30	6.24E-01(1.31E-01)	8.78E-01(1.56E-01)+	8.93E-01(1.87E-01)+	1.05E+01(1.08)+	9.5(8E-01)+
	50	8.28E-01(1.35E-01)	1.09(1.72E-01)+	1.01(1.69E-01)+	1.21E+01(8.92E-01)+	1.16E+01(5.93E-01)+
	100	9.73E-01(3.76E-01)	1.19(2.03E-01)+	1.26(2.47E-01)+	1.43E+01(7.26E-01)+	1.42E+01(4.16E-01)+
	10	1.4E-01(1.5E-01)	6.12E-01(1.91E-01)+	4.94E-02(1.9E-02)-	5.16E+02(1.23E+02)+	3.33E+01(8.34)+
f_{13}	30	7.69E-01(2.07E-01)	1.11(4.2E-01)+	1.03(4.02E-01)+	4.12E+02(4.94E+01)+	3.65E+02(3.05E+01)+
	50	1.11(1.64)	1.43(5.55E-01)+	1.39(5.43E-01)+	6.88E+02(7.28E+01)+	6.71E+02(4.64E+01)+
	100	6.51E+01(2.6E+01)	4.21(2.01)-	6.72E+01(3.14E+01)+	1.71E+03(1.21E+02)+	1.66E+03(8.09E+01)+
	10	4.71E-01(1.37E-01)	5.53(1.16)+	7.55E-01(2.39E-01)+	1.49E+05(1.37E+05)+	2.24E+04(1.55E+04)+
	30	2.09E+01(6.07)	2.7E+01(3.05)+	2.76E+01(3.43)+	2.4E+07(1.1E+07)+	1.1E+07(4.02E+06)+
f_{14}	50	6.53E+01(4.09E+01)	6.21E+01(7.65)-	6.2E+01(7.59)-	1.4E+08(7.8E+07)+	8.1E+08(2.1E+07)+
	100	1.71E+04(1.01E+04)	2.35E+03(1.27E+03)-	7.04E+01(1.58E+01)-	6.7E+08(1.8E+08)+	4.8E+08(9.7E+07)+

Table 1 continued

<i>f</i>	<i>D</i>	AHFADE Mean (STD) Sign	SHADE	jDE	FA	LFA
<i>f</i> ₁₆	10	4.09E-01(7.23E-01)	4.16(2.27E-01)+	1.45(5.3E-01)+	3.98(1.2E-01)+	3.73(1.02E-01)+
	30	1.33E+01(8.73E-01)	1.4E+01(2.2E-01)+	1.04E+01(7.45E-01)-	1.35E+01(1.29E-01)≈	1.33E+01(2E-01)≈
	50	2.35E+01(4.96E-01)	2.38E+01(2.78E-01)+	2.07E+01(8.18E-01)-	2.32E+01(1.39E-01)-	2.31E+01(1.52E-01)-
	100	4.81E+01(4.06E-01)	4.84E+01(3.03E-01)+	4.57E+01(5.07E-01)-	4.74E+01(1.82E-01)-	4.74E+01(2.57E-01)-
<i>f</i> ₁₇	10	2.67E+02(1.77E+02)	3.23E+04(3.64E+04)+	1.25E+03(1.04E+03)+	8.58E+06(8.19E+06)+	4.86E+04(3.26E+04)+
	30	2.58E+05(1.25E+05)	2E+07(9E+06)+	2.43E+05(1.66E+05)≈	3.2E+08(1.7E+08)+	6.2E+07(2.2E+07)+
	50	1.2E+06(2E+06)	4.07E+07(1.84E+07)+	1.3E+06(2E+06)≈	1.2E+09(4.6E+08)+	4.5E+08(9.1E+07)+
	100	4.5E+06(1.39E+06)	1.81E+08(5.5E+07)+	4.52E+06(1.41E+06)≈	3.7E+09(7.1E+08)+	2.2E+09(3.6E+08)+
<i>f</i> ₁₈	10	1.158(7.4E-01)	2.2E+03(2.99E+03)+	2.2E+03(3.47E+03)+	1.39E+08(1.61E+08)+	9.25E+04(1.95E+05)+
	30	9.86E+01(1.06E+02)	5E+06(3E+06)+	5.94E+03(5.42E+03)+	8.8E+09(2.9E+09)+	5E+09(1.3E+09)+
	50	5.98E+04(3.61E+05)	3.77E+06(2.18E+06)+	3.46E+06(2.01E+06)+	2.9E+10(5.9E+09)+	2.3E+10(3.9E+09)+
	100	5.3E+07(3.5E+07)	1.8E+07(5.7E+06)-	6.78E+07(4.29E+07)+	8.1E+10(9.4E+09)+	7.4E+10(6.4E+09)+
<i>f</i> ₁₉	10	1.55(7.88E-01)	3.63(6.7E-01)+	9.32E-01(7.9E-01)-	6.49E+01(3.39E+01)+	1.33E+01(4.16)+
	30	1.48E+01(1.73E+01)	1.49E+01(2.25)+	1.53E+01(2.36)+	1.19E+03(4.06E+02)+	6.72E+02(1.27E+02)+
	50	6.73E+01(1.9E+01)	6.65E+01(1.13E+01)≈	6.72E+01(2.06E+01)≈	5.51E+03(1.81E+03)+	3.21E+03(6.23E+02)+
	100	2.71E+02(5.41E+01)	1.88E+02(1.87E+01)-	2.71E+02(5.56E+01)≈	2.1E+04(4.9E+03)+	1.69E+04(2.22E+03)+
<i>f</i> ₂₀	10	3.72E-01(4.12E-01)	3.87E+01(1.72E+01)+	2.78(1.63)+	2.3E+06(5.31E+06)+	2.85E+03(2.16E+03)+
	30	2.46E+03(1.08E+03)	1.63E+05(1.69E+05)+	1.25E+02(4.18E+01)-	9.86E+06(1.2E+07)+	1.44E+05(8.07E+04)+
	50	7.07E+03(1.5E+03)	7.79E+05(7.51E+05)+	7.96E+05(7.78E+05)+	1.3E+07(8.94E+06)+	7.56E+05(3.65E+05)+
	100	2.19E+04(4.08E+03)	3.11E+06(2.13E+06)+	3.46E+06(2.29E+06)+	5E+07(2.7E+07)+	8.21E+06(2.92E+06)+
<i>f</i> ₂₁	10	6.43E-02(1.21E-01)	1.38E+03(6.52E+02)+	2.52E+01(4.15E+01)+	2.51E+06(3.46E+06)+	5.24E+03(2.91E+03)+
	30	5.25E+04(2.56E+04)	4E+06(4E+06)+	6.3E+04(5.68E+04)≈	1.4E+08(7.8E+07)+	1.7E+07(8.19E+06)+
	50	6.4E+05(2.18E+05)	2.8E+07(1E+07)+	7.1E+05(6E+05)≈	4.5E+08(1.7E+08)+	1E+08(3E+07)+
	100	4.44E+06(1.32E+06)	1.2E+08(4.8E+07)+	4.43E+06(1.57E+06)≈	1.8E+09(3.8E+08)+	9E+08(1.5E+08)+
<i>f</i> ₂₂	10	1.56E+01(9.44)	1.25E+02(8.8E+01)+	5.75(9.01)-	5.14E+02(1.24E+02)+	1.07E+02(3.14E+01)+
	30	2.38E+02(1.56E+02)	1.32E+03(2.54E+02)+	2.2E+02(1.18E+02)≈	2.44E+04(6.53E+04)+	2.21E+03(5.28E+02)+
	50	1.99E+03(5.98E+02)	2.79E+03(3.19E+02)+	2.63E+03(3.04E+02)+	6.34E+05(6.57E+05)+	5.89E+04(4.3E+04)+
	100	5.83E+03(3.26E+02)	6.23E+03(4.9E+02)+	6.44E+03(5.02E+02)+	2.27E+06(1.26E+06)+	7.12E+05(2.86E+05)+

Table 1 continued

f	D	AHFADE Mean (STD) Sign	SHADE	jDE	FA	LFA
f_{23}	10	-4.03E+02(1.2E-11)	-4.03E+02(6.01E-03)+	-4.03E+02(2.57E-13)-	-1.2E+02(1.39E+02)+	-3.09E+02(2.37E+01)+
	30	-7.01E+03(2.03)	-7.01E+03(7.04E-01)+	-7.02E+03(1.05E-01)-	-5.39E+03(4.7E+02)+	-5.91E+03(2.27E+02)+
	50	-5.05E+03(1.06E+01)	-5.06E+03(1.59)-	-5.05E+03(5.8E-01)-	-1.37E+03(7.65E+02)+	-2.31E+03(4.4E+02)+
	100	-7.02E+03(4.93E+01)	-7.09E+03(1.76E+01)-	-7.18E+03(2.08)-	1.71E+03(1.18E+03)+	8.18E+02(9.27E+02)+
f_{24}	10	-1.9E+02(5.27)	-1.34E+02(9.57)+	-1.86E+02(3.22)+	-6.12E+01(1.21E+01)+	-1.07E+02(1.01E+01)+
	30	-3.86E+02(6.67)	-3.88E+02(3.31)-	-3.97E+02(5.87)-	-8.58E+01(3.19E+01)+	-1.16E+02(2.39E+01)+
	50	-8.66E+02(8.74)	-8.66E+02(2.91)≈	-8.86E+02(5.39)-	-2.43E+02(6.97E+01)+	-2.88E+02(3.46E+01)+
	100	-1.66E+03(2.86E+01)	-1.69E+03(5.73)-	-1.76E+03(5.13)-	-2.14E+02(1.2E+02)+	-2.52E+02(8.48E+01)+
f_{25}	10	-1.38E+02(3.18E+01)	-1.21E+02(7.93)+	-1.37E+02(3.44E+01)≈	-1.03E+02(6.7)+	-1.22E+02(7.12)+
	30	-6.48E+02(2.00)	-6.27E+02(5.12)+	-6.48E+02(1.89)≈	-4.5E+02(5.94E+01)+	-5.38E+02(1.71E+01)+
	50	-8.39E+02(6.68)	-7.99E+02(8.19)+	-7.54E+02(8.07)+	-3.35E+02(1.16E+02)+	-4.85E+02(4.9E+01)+
	100	-1.27E+03(2.26E+01)	-1.25E+03(1.76E+01)+	-1.23E+03(1.51E+01)+	1.91E+02(2.08E+02)+	-7.88E+01(1.17E+02)+
f_{26}	10	-7.92E+02(1.4E-01)	-7.91E+02(1.56E-01)+	-7.92E+02(4.69E-02)-	-7.87E+02(1.32)+	-7.89E+02(4.8E-01)+
	30	-2.25E+03(4.28E+01)	-2.26E+03(3.66E-01)+	-2.25E+03(3.82E+01)-	-2.07E+03(1.22E+02)+	-2.25E+03(6.6)+
	50	-2.77E+03(5.77E+01)	-2.76E+03(6.77E+01)≈	-2.76E+03(8.99E+01)≈	-2.2E+03(1.78E+02)+	-2.65E+03(9.15E+01)+
	100	-2.6E+03(5.54)	-2.57E+03(1.19E+01)+	-2.6E+03(5.71)≈	-1.2E+03(2.52E+02)+	-1.42E+03(1.16E+02)+
f_{27}	10	-3.14E+03(1.88E+02)	-3.14E+03(1.91E+02)≈	-3.14E+03(1.74E+02)≈	-2.74E+03(9.57E+01)+	-2.99E+03(7.76E+01)+
	30	-7.38E+03(1.07E+02)	-7.14E+03(1.69E+02)+	-7.39E+03(8.57E+01)≈	-6.02E+03(1.7E+02)+	-6.6E+03(1.78E+02)+
	50	-1.02E+04(8.56E+01)	-9.64E+03(1.76E+02)+	-1.02E+04(1.05E+02)+	-7.91E+03(3.56E+02)+	-8.37E+03(1.02E+02)+
	100	-1.51E+04(2.32E+02)	-1.41E+04(1.98E+02)+	-1.43E+04(1.74E+02)+	-9.61E+03(9.75E+02)+	-1.08E+04(2.4E+02)+
f_{28}	10	-6.01E+03(6.02E+01)	-6.03E+03(8.24E+01)≈	-6.03E+03(7.44E+01)≈	-4.8E+03(2.98E+02)+	-5.57E+03(9.42E+01)+
	30	-1.8E+04(2.03E+02)	-1.79E+04(8.18E+01)+	-1.81E+04(2.06E+02)≈	-1.09E+04(7.75E+02)+	-1.37E+04(2.88E+02)+
	50	-2.21E+04(4.67E+02)	-2.21E+04(3.35E+02)≈	-2.21E+04(3.38E+02)≈	-7.53E+03(1.44E+03)+	-1.21E+04(7.54E+02)+
	100	-5.19+04(9.31E+02)	-4.97E+04(3.09E+03)+	-5.19E+04(9.02E+02)≈	-1.84E+04(2.62E+03)+	-2.55E+04(1.33E+03)+
f_{29}	10	-1E+09(3.62E+01)	-1E+09(3.74E+06)+	-1E+09(9.07E+05)+	-9.9E+08(1.76E+07)+	-1E+09(6.24E+04)+
	30	-5.95E+09(2.37E+06)	-6E+09(1.15E+05)+	-5.9E+09(6.3E+06)≈	-5.2E+09(2.1E+08)+	-5.6E+09(6.7E+07)+
	50	-7E+09(6.33E+06)	-7.4E+09(7.32E+05)-	-7E+09(3E+07)+	-4.8E+09(5.2E+08)+	-5.7E+09(1.7E+08)+
	100	-3E+10(1.1E+08)	-3E+10(1.17E+06)-	-2E+10(1.17E+09)+	-2E+10(1.3E+09)+	-2E+10(4.5E+08)+
f_{30}	10	-4.4E+08(1.64E+01)	-4.4E+08(3.24E+02)+	-4.4E+08(2.11E+02)+	-4.4E+08(2.03E+05)+	-4.4E+08(1.86E+03)+
	30	-6E+07(1.03E+03)	-6.5E+07(1.4E+04)+	-6E+07(1.38E+03)≈	-5.3E+07(4.08E+06)+	-6.2E+07(8.95E+05)+
	50	-6E+08(2.33E+04)	-6.1E+08(5.9E+04)+	-6E+08(6.2E+04)≈	-5.5E+08(1.9E+07)+	-5.9E+08(4.67E+06)+
	100	-3E+09(5.27E+05)	-3E+09(1.18E+06)+	-3E+09(1.74E+06)+	-2E+09(1.6E+08)+	-3E+09(4.6E+07)+

Table 2 Results of the Wilcoxon test between AHFADE and other considered algorithms using CEC2014 for $D = 10, 30, 50$ and 100

D	Algorithms	R^+	R^-	p value	+	≈	-	Dec.
10	AHFADE versus SHADE	443	22	0.000	28	2	0	+
	AHFADE versus jDE	316.5	148.5	0.101	17	4	9	≈
	AHFADE versus FA	465	0	0.000	30	0	0	+
	AHFADE versus LFA	465	0	0.000	30	0	0	+
30	AHFADE versus SHADE	349.5	115.5	0.017	27	1	2	+
	AHFADE versus jDE	263	202	0.590	14	9	7	≈
	AHFADE versus FA	464	1	0.000	28	2	0	+
	AHFADE versus LFA	424.5	40.5	0.000	27	2	1	+
50	AHFADE versus SHADE	325	140	0.067	19	5	6	≈
	AHFADE versus jDE	288.5	176.5	0.252	14	6	10	≈
	AHFADE versus FA	453	12	0.000	26	1	3	+
	AHFADE versus LFA	447	18	0.000	26	0	4	+
100	AHFADE versus SHADE	289.5	175.5	0.273	16	4	10	≈
	AHFADE versus jDE	268.5	196.5	0.487	15	5	10	≈
	AHFADE versus FA	453	12	0.000	26	0	4	+
	AHFADE versus LFA	447	18	0.000	26	0	4	+

Table 3 Average ranks computed through the Friedman test for all considered algorithms across all functions and over all dimensions using CEC2014, at the significance level 0.05

Algorithm	10D	30D	50D	100D	Mean ranking	Rank
AHFADE	1.500	1.800	1.916	2.083	1.825	1
jDE	<u>1.800</u>	<u>2.133</u>	<u>1.983</u>	<u>2.100</u>	<u>2.004</u>	2
SHADE	3.216	2.750	2.866	2.566	2.850	3
FA	3.700	3.616	3.616	3.666	3.650	4
LFA	4.783	4.700	4.616	4.583	4.670	5
Friedman p value	0.0000	0.0000	0.0000	0.0000		

10.2 Localization performance

This section presents the simulation results of the proposed AHFADE algorithm and the well-known algorithms such as SDP, DE and FA, which are performed to verify and compare their performance under the same noisy environment. In the following simulations, the CRLB is employed as a benchmark for evaluating the RMSE performance of the considered algorithms.

The numerical simulations are conducted for the passive target localization system in LOS environment, which consists of one transmitter, four receivers located at known positions and the passive target located at different positions. The evaluation should show how sensitive is performance of all considered algorithms under the noisy TOA measurements. Besides, this work demonstrates the influence of changing the position of the target with respect to the geometry of transmitter and receivers on the localization performance of the existing algorithms.

In this regard, three simulation scenarios are conducted here based on different positions of the target such as: i) the true position of the target lies inside the convex hull of the

four receivers; ii) the position of the target is outside of the convex hull of the four receivers; iii) the position of the target is randomly deployed in the $200\text{m} \times 200\text{m}$ square area, and its position varies for each simulation run.

For the proposed passive target localization system, each simulation scenario has the same configuration with transmitter which is located at the origin of the coordinate system and the four receivers forming the convex hull, at: $\mathbf{x}_1^r = [100 \ 100]^T \text{m}$, $\mathbf{x}_2^r = [100 \ -100]^T \text{m}$, $\mathbf{x}_3^r = [-100 \ -100]^T \text{m}$, and $\mathbf{x}_4^r = [-100 \ 100]^T \text{m}$.

In this way, the localization accuracy is evaluated in terms of RMSE, which can be defined as follows:

$$\text{RMSE} = \sqrt{\frac{1}{N_m} \sum_{n=1}^{N_m} \|\hat{\mathbf{x}}^{(n)} - \mathbf{x}\|_2^2}, \tag{61}$$

where \mathbf{x} is the true target position, $\hat{\mathbf{x}}^{(n)}$ is the estimated target position and N_m is the number of simulation runs for a given variance of the noise σ_{ni}^2 . A Monte Carlo simulation, which consists of $N_m = 1000$ runs, is conducted to determine the RMSE performance of the considered algorithms.

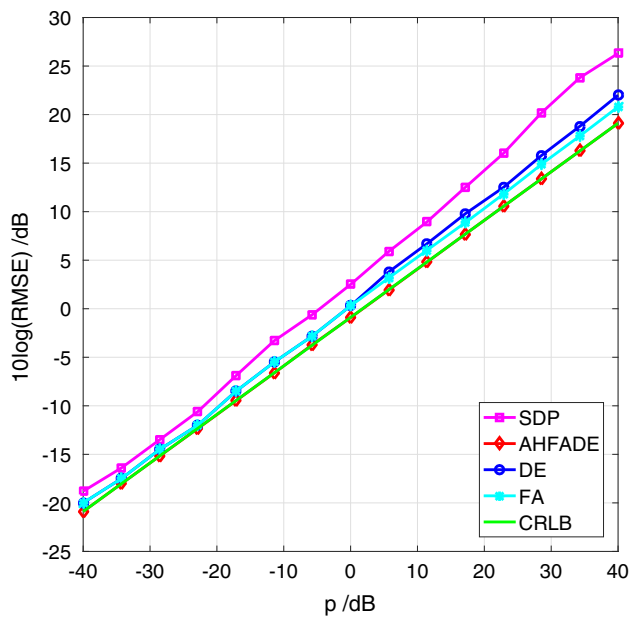


Fig. 6 RMSE curves in terms of p of the considered algorithms for the first simulation scenario

Figure 6 shows the simulation results of the comparison between CRLB and the RMSEs of all considered algorithms as a function of the measurement noise $p = 10 \log(\sigma_{ni}^2)$, for the first simulation scenario, when the true position of the target is located at $\mathbf{x} = [20 \ 30]^T$ m.

As shown in Fig. 6, it can be observed that the RMSE of the proposed AHFADE algorithm attains the CRLB accuracy for all the considered range of p . Furthermore, from this figure it should be noted that the SDP, FA and DE algorithms can achieve performance several dBs above the CRLB. However, numerical results of this simulation show that the SDP method has significant deviation from the CRLB for high values of p (i.e., $p > 20$ dB), compared with other algorithms.

Figure 7 shows the results of the comparison between CRLB and the RMSEs of all considered algorithms in terms of measurement noise p for the second simulation scenario, when the true position of target is located at $\mathbf{x} = [120 \ 100]^T$ m.

From Fig. 7, it is observed that the proposed AHFADE algorithm can attain the CRLB accuracy in Gaussian noise environment and outperforms all other considered algorithms as p increases. The simulation results also show that the FA and DE algorithms have degradation of localization performance compared to the proposed AHFADE algorithm. It can be also observed that the SDP method has the worst performance, especially when the measurement noise becomes very large (i.e., $p \geq 30$ dB).

Figure 8 shows the results of comparison between CRLB and the RMSEs of all considered algorithms in terms of measurement noise p for the third simulation scenario, where the

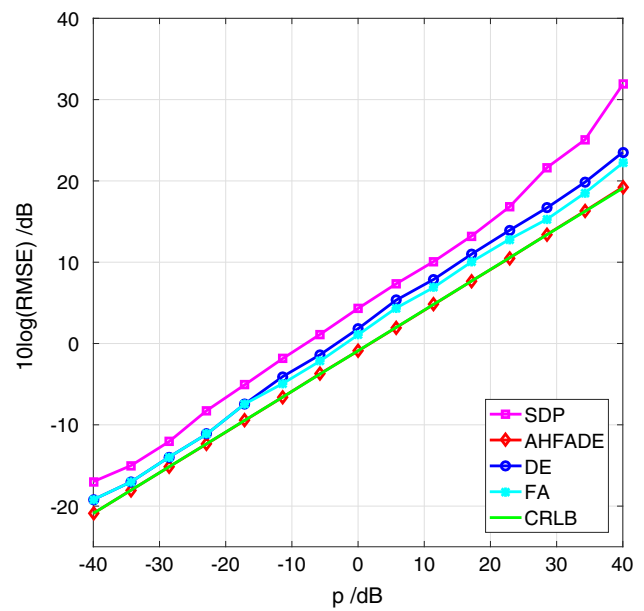


Fig. 7 RMSE curves in terms of p of the considered algorithms for the second simulation scenario

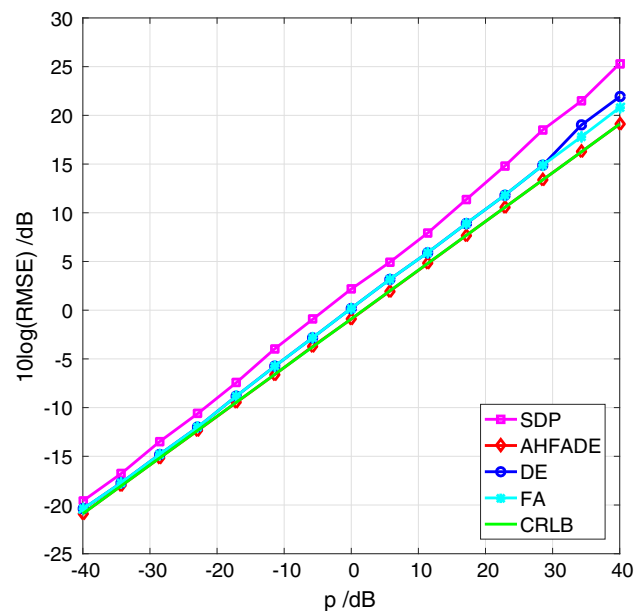


Fig. 8 RMSE curves in terms of the p of the considered algorithms for the third simulation scenario

true position of the passive target is randomly located within the considered area for each simulation run.

As it could be expected, the results show that the proposed AHFADE algorithm attains the CRLB accuracy for all the considered range of p , and provides superior performance over the FA, DE and SDP algorithms, as shown in Fig. 8.

The comparison between numerical results of the above three simulation scenarios, clearly shows that the RMSE of each considered algorithm is lowest when the true position

Table 4 The average computational time of the considered algorithms

	SDP	AHFADE	DE	FA
Scenario 1	0.737	0.0389	0.0116	0.0115
Scenario 2	0.7751	0.027	0.0091	0.009
Scenario 3	0.79	0.0419	0.011	0.01

of the target lies inside the convex hull of the four receivers. On the other hand, the obtained RMSEs of all the considered algorithms are highest when the position of the target is outside of the convex hull of the four receivers. It should be noticed that the proposed AHFADE algorithm has the best performance and its RMSE attains the CRLB accuracy for all the considered range of p in every considered scenario. However, the RMSE performance of the SDP method rapidly deviates from the CRLB, especially in the presence of significant measurement noise.

The average computational time in searching the global optimal solution of each algorithm is another important factor that has a strong influence on the localization performance. To this aim, the average time consumed to obtain the global optimal solution of the considered algorithms can be determined on the same computer with 3.2 GHz CPU and 16 GB of RAM. Based on the proposed simulation scenarios, Table 4 shows the corresponding average computational time to achieve the global optimal solution taken by each algorithm to satisfy the stopping condition.

It can be seen from Table 4 that the SDP method has the highest average computation time among all examined algorithms, while the FA and DE algorithms have the best average execution time. Generally, it can be concluded that the AHFADE algorithm achieves the best trade-off between the benefit of the localization accuracy and computational complexity, and in this way becomes attractive for applications in sensor networks in noisy environment.

In order to further evaluate the localization performance, the cumulative distribution functions (CDFs) of localization errors of the considered algorithms are conducted for measurement noise $\sigma_{ni}^2 = 1 \text{ m}^2$. The localization error (LE) is defined as the Euclidean distance between the estimated and the true position of the passive target, i.e.,

$$LE = \|\hat{\mathbf{x}}^{(n)} - \mathbf{x}\|_2, \forall n \in \{1, \dots, N_m\}. \tag{62}$$

Figure 9 represents the simulation results for the second scenario with the corresponding CDFs in terms of localization error obtained for each algorithm.

From Fig. 9, it is observed that the proposed AHFADE algorithm provides the lowest localization error compared to the other considered algorithms. Additionally, it is evident that the AHFADE algorithm has localization error less than

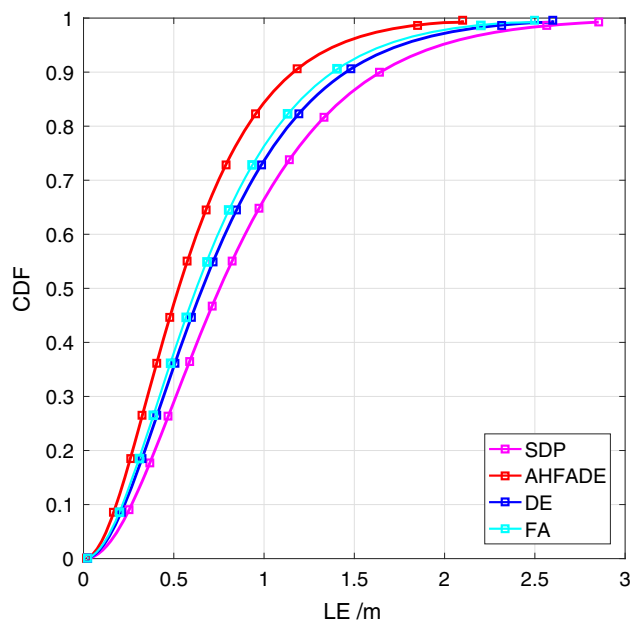


Fig. 9 CDFs of passive target localization error of the considered algorithms for the second simulation scenario

1.18 m in 90% of the cases, while the FA, DE and SDP have localization error less than 1.4 m, 1.45 m and 1.64 m, respectively. Therefore, the proposed AHFADE algorithm has smaller localization error in terms of CDFs compared to other considered algorithms.

Finally, the influence of the number of receivers N at known positions on the localization accuracy of all algorithms is also considered in this section. In this context, the corresponding coordinates of the i th receiver can be obtained as follows:

$$\mathbf{x}_i^r = \begin{bmatrix} R \cos \varphi_i \\ R \sin \varphi_i \end{bmatrix}, \quad \forall i \in \{1, \dots, N\}, \tag{63}$$

where $R = 100\sqrt{2}$ m is the radius of the circle and the angular separation between receivers can be expressed as $\varphi_i = 2\pi/i$.

Hence, Fig. 10 depicts the RMSE curves of all considered algorithms as a function of the number of receivers N , for the first simulation scenario where the target position is set at $\mathbf{x} = [20 \ 30]^T \text{ m}$ inside the convex hull of receivers, when the variance of measurement noise is $\sigma_{ni}^2 = 1 \text{ m}^2$.

As can be seen from Fig. 10, by increasing the number of receivers from 4 to 10, the RMSEs of all considered algorithms significantly decreased. As shown, the proposed AHFADE algorithm can achieve the CRLB under the given noise environment. It can also be noticed that with increasing the number of receivers from 4 to 12, the proposed AHFADE algorithm provided approximately 42.77% improvement in localization accuracy.

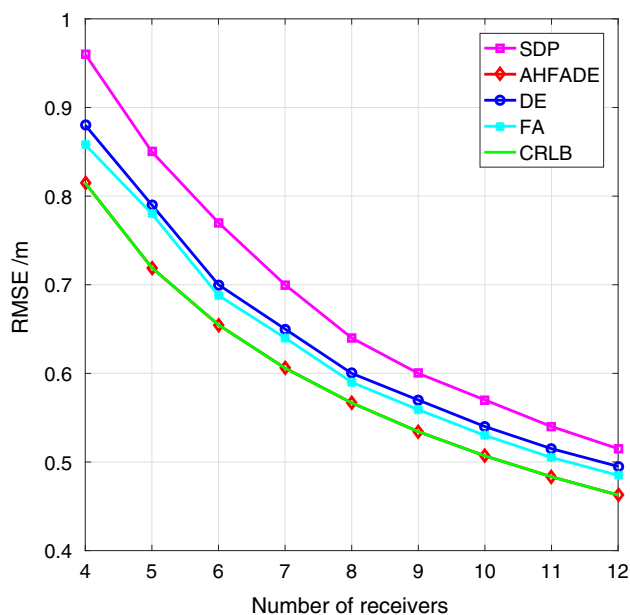


Fig. 10 RMSEs of the considered algorithms as function of the number of receivers

Based on the above obtained simulation results, it can be concluded that the performance of the proposed AHFADE algorithm shows better robustness to measurement noise than all other considered algorithms in solving the passive target localization problem.

11 Conclusion

In this paper, the passive target localization problem based on the noisy TOA measurements, utilizing multiple receivers and a single transmitter, has been considered and investigated. In this context, an improved robust AHFADE algorithm has been proposed, based on the hybridization of DE and FA, to solve this nonlinear and non-convex localization problem with high accuracy even in highly noisy environments. In the proposed algorithm, a dynamically adapted parameter has been introduced to select the appropriate mutation operator for achieving a proper balance between global exploration and local exploitation during the evolution process. Moreover, the crossover and selection operators of DE algorithm are incorporated into FA, where the control parameters of both DE and FA are dynamically adjusted during the evolution process. To evaluate the performance of the proposed algorithm, the CRLB for the passive target localization problem has been derived. In addition, to compare the optimization performance, the statistical analysis has been conducted between AHFADE and several well-known algorithms on CEC2014 benchmark test problems.

From the numerical results of statistical comparison between AHFADE algorithm and other well-known algorithms, such as SHADE, jDE, FA and LFA, it can be concluded that the hybridization proposed in this paper can improve the overall optimization performance, especially compared to the individual optimization performance of SHADE and FA algorithms. Furthermore, simulation results have shown that the proposed AHFADE algorithm exhibits better robustness in high-noise environments and provides better localization performance in comparison with well-known algorithms such as SDP, DE and FA. Additionally, the results have shown that the AHFADE algorithm can attain the CRLB accuracy and is robust against changes in the topology. Finally, the AHFADE algorithm can provide a proper balance between localization accuracy and computational complexity, thus making it more attractive for applications in sensor networks in noisy environment.

In the future research, the focus will be on the problem of finding the optimal geometry of the receiver configuration for the passive target localization in the presence of non-line-of-sight (NLOS) propagation. In addition, the research can be extended to parameter sensitivity analysis and influence of parameter variations during the evolution process to further enhance the optimization performance for the given localization problem.

Acknowledgements The work of M. Simić was supported in part by Serbian Ministry of Education and Science under Grant TR32028.

Compliance with ethical standards

Conflict of interest Author Maja Rosić declares that she has no conflict of interest. Author Mirjana Simić declares that she has no conflict of interest. Author Predrag Pejović declares that he has no conflict of interest.

Ethical approval This article does not contain any studies with human participants or animals performed by any of the authors.

A Derivation of CRLB

From Eq. (8), the first partial derivative of the log-likelihood function with respect to \mathbf{x} is given as:

$$\begin{aligned} & \frac{\partial \ln \left(f \left(\tilde{\mathbf{d}} | \mathbf{x} \right) \right)}{\partial \mathbf{x}} \\ &= -\frac{1}{2} \frac{\partial}{\partial \mathbf{x}} \left(\left(\tilde{\mathbf{d}} - \mathbf{d}(\mathbf{x}) \right)^T \mathbf{C}^{-1} \left(\tilde{\mathbf{d}} - \mathbf{d}(\mathbf{x}) \right) \right), \end{aligned} \quad (64)$$

where

$$\begin{aligned} & \frac{\partial}{\partial \mathbf{x}} \left((\tilde{\mathbf{d}} - \mathbf{d}(\mathbf{x}))^T \mathbf{C}^{-1} (\tilde{\mathbf{d}} - \mathbf{d}(\mathbf{x})) \right) \\ &= -2 \frac{\partial \mathbf{d}(\mathbf{x})^T}{\partial \mathbf{x}} \mathbf{C}^{-1} (\tilde{\mathbf{d}} - \mathbf{d}(\mathbf{x})). \end{aligned} \tag{65}$$

Then, Eq. (64) can be expressed as:

$$\frac{\partial \ln(f(\tilde{\mathbf{d}}|\mathbf{x}))}{\partial \mathbf{x}} = \frac{\partial \mathbf{d}(\mathbf{x})^T}{\partial \mathbf{x}} \mathbf{C}^{-1} (\tilde{\mathbf{d}} - \mathbf{d}(\mathbf{x})). \tag{66}$$

Hence, taking the partial derivative with respect to x follows:

$$\frac{\partial \ln(f(\tilde{\mathbf{d}}|\mathbf{x}))}{\partial x} = \frac{\partial \mathbf{d}(\mathbf{x})^T}{\partial x} \mathbf{C}^{-1} (\tilde{\mathbf{d}} - \mathbf{d}(\mathbf{x})). \tag{67}$$

Then, the first diagonal element of the FIM can be derived as follows:

$$\begin{aligned} I_{xx} &= E \left[\left(\frac{\partial \ln(f(\tilde{\mathbf{d}}|\mathbf{x}))}{\partial x} \right) \left(\frac{\partial \ln(f(\tilde{\mathbf{d}}|\mathbf{x}))}{\partial x} \right)^T \right] \\ &= E \left[\left(\frac{\partial \mathbf{d}(\mathbf{x})}{\partial x} \right)^T \mathbf{C}^{-1} (\tilde{\mathbf{d}} - \mathbf{d}(\mathbf{x})) (\tilde{\mathbf{d}} - \mathbf{d}(\mathbf{x}))^T \right. \\ &\quad \left. (\mathbf{C}^{-1})^T \left(\frac{\partial \mathbf{d}(\mathbf{x})}{\partial x} \right) \right] \\ &= \left(\frac{\partial \mathbf{d}(\mathbf{x})}{\partial x} \right)^T \mathbf{C}^{-1} E[\mathbf{nn}^T] (\mathbf{C}^{-1})^T \left(\frac{\partial \mathbf{d}(\mathbf{x})}{\partial x} \right) \\ &= \left(\frac{\partial \mathbf{d}(\mathbf{x})}{\partial x} \right)^T (\mathbf{C}^{-1})^T \left(\frac{\partial \mathbf{d}(\mathbf{x})}{\partial x} \right). \end{aligned} \tag{68}$$

The remaining elements of the FIM can be derived in the same way as above:

$$\begin{aligned} I_{xy} = I_{yx} &= E \left[\left(\frac{\partial \ln(f(\tilde{\mathbf{d}}|\mathbf{x}))}{\partial x} \right) \left(\frac{\partial \ln(f(\tilde{\mathbf{d}}|\mathbf{x}))}{\partial y} \right)^T \right] \\ &= \left(\frac{\partial \mathbf{d}(\mathbf{x})}{\partial x} \right)^T (\mathbf{C}^{-1})^T \left(\frac{\partial \mathbf{d}(\mathbf{x})}{\partial y} \right), \end{aligned} \tag{69}$$

$$\begin{aligned} I_{yy} &= E \left[\left(\frac{\partial \ln(f(\tilde{\mathbf{d}}|\mathbf{x}))}{\partial y} \right) \left(\frac{\partial \ln(f(\tilde{\mathbf{d}}|\mathbf{x}))}{\partial y} \right)^T \right] \\ &= \left(\frac{\partial \mathbf{d}(\mathbf{x})}{\partial y} \right)^T (\mathbf{C}^{-1})^T \left(\frac{\partial \mathbf{d}(\mathbf{x})}{\partial y} \right). \end{aligned} \tag{70}$$

According to Eq. (4), the partial derivative of $\mathbf{d}(\mathbf{x})$ with respect to the components of \mathbf{x} can be expressed as:

$$\frac{\partial \mathbf{d}(\mathbf{x})}{\partial \mathbf{x}} = \begin{bmatrix} \frac{x-x_1^r}{\|\mathbf{x}-\mathbf{x}_1^r\|_2} + \frac{x}{\|\mathbf{x}\|_2} & \frac{y-y_1^r}{\|\mathbf{x}-\mathbf{x}_1^r\|_2} + \frac{y}{\|\mathbf{x}\|_2} \\ \frac{x-x_2^r}{\|\mathbf{x}-\mathbf{x}_2^r\|_2} + \frac{x}{\|\mathbf{x}\|_2} & \frac{y-y_2^r}{\|\mathbf{x}-\mathbf{x}_2^r\|_2} + \frac{y}{\|\mathbf{x}\|_2} \\ \vdots & \vdots \\ \frac{x-x_N^r}{\|\mathbf{x}-\mathbf{x}_N^r\|_2} + \frac{x}{\|\mathbf{x}\|_2} & \frac{y-y_N^r}{\|\mathbf{x}-\mathbf{x}_N^r\|_2} + \frac{y}{\|\mathbf{x}\|_2} \end{bmatrix}, \tag{71}$$

where $\partial \mathbf{d}(\mathbf{x}) / \partial \mathbf{x}$ is the $N \times 2$ Jacobian matrix.

Performing the matrix multiplication, the following expressions can be easily obtained

$$\begin{aligned} I_{xx} &= \left(\frac{\partial \mathbf{d}(\mathbf{x})}{\partial x} \right)^T (\mathbf{C}^{-1})^T \left(\frac{\partial \mathbf{d}(\mathbf{x})}{\partial x} \right) \\ &= \sum_{i=1}^N \frac{1}{\sigma_{ni}^2} \left(\frac{x-x_i^r}{\|\mathbf{x}-\mathbf{x}_i^r\|_2} + \frac{x}{\|\mathbf{x}\|_2} \right)^2. \end{aligned} \tag{72}$$

Similarly, the expressions for the remaining elements of FIM can be obtained as:

$$\begin{aligned} I_{xy} = I_{yx} &= \left(\frac{\partial \mathbf{d}(\mathbf{x})}{\partial x} \right)^T (\mathbf{C}^{-1})^T \left(\frac{\partial \mathbf{d}(\mathbf{x})}{\partial y} \right) \\ &= \sum_{i=1}^N \frac{1}{\sigma_{ni}^2} \left(\frac{x-x_i^r}{\|\mathbf{x}-\mathbf{x}_i^r\|_2} + \frac{x}{\|\mathbf{x}\|_2} \right) \left(\frac{y-y_i^r}{\|\mathbf{x}-\mathbf{x}_i^r\|_2} + \frac{y}{\|\mathbf{x}\|_2} \right), \end{aligned} \tag{73}$$

$$\begin{aligned} I_{yy} &= \left(\frac{\partial \mathbf{d}(\mathbf{x})}{\partial y} \right)^T (\mathbf{C}^{-1})^T \left(\frac{\partial \mathbf{d}(\mathbf{x})}{\partial y} \right) \\ &= \sum_{i=1}^N \frac{1}{\sigma_{ni}^2} \left(\frac{y-y_i^r}{\|\mathbf{x}-\mathbf{x}_i^r\|_2} + \frac{y}{\|\mathbf{x}\|_2} \right)^2. \end{aligned} \tag{74}$$

Finally, Eqs. (55)-(57) of the corresponding elements of FIM are obtained.

References

Alweshah M, Abdullah S (2015) Hybridizing firefly algorithms with a probabilistic neural network for solving classification problems. *Appl Soft Comput* 35:513–524

Arora JS (2004) *Introduction to optimum design*. Elsevier, Amsterdam

Asmaa L, Hatim KA, Abdelaaziz M (2014) Localization algorithms research in wireless sensor network based on multilateration and trilateration techniques. In: 2014 3rd IEEE international colloquium in information science and technology (CIST), IEEE, pp 415–419

Awad NH, Ali MZ, Mallipeddi R, Suganthan PN (2018) An improved differential evolution algorithm using efficient adapted surrogate model for numerical optimization. *Inf Sci* 451:326–347

Aydilek IB (2018) A hybrid firefly and particle swarm optimization algorithm for computationally expensive numerical problems. *Appl Soft Comput* 66:232–249

- Baraldi P, Cannarile F, Di Maio F, Zio E (2016) Hierarchical k-nearest neighbours classification and binary differential evolution for fault diagnostics of automotive bearings operating under variable conditions. *Eng Appl Artif Intell* 56:1–13
- Bishop AN, Fidan B, Anderson BD, Doğançay K, Pathirana PN (2010) Optimality analysis of sensor-target localization geometries. *Automatica* 46(3):479–492
- Biswas P, Liang TC, Toh KC, Ye Y, Wang TC (2006) Semidefinite programming approaches for sensor network localization with noisy distance measurements. *IEEE Trans Autom Sci Eng* 3(4):360–371
- Boyd S, Vandenberghe L (2004) *Convex optimization*. Cambridge University Press, Cambridge
- Brest J, Greiner S, Boskovic B, Mernik M, Zumer V (2006) Self-adapting control parameters in differential evolution: a comparative study on numerical benchmark problems. *IEEE Trans Evol Comput* 10(6):646–657
- Cakir O, Kaya I, Yazgan A, Cakir O, Tugcu E (2014) Emitter location finding using particle swarm optimization. *Radioengineering* 23(1):252–258
- Chalise BK, Zhang YD, Amin MG, Himed B (2014) Target localization in a multi-static passive radar system through convex optimization. *Signal Processing* 102:207–215
- Chan FK, So HC, Ma WK, Lui KW (2013) A flexible semi-definite programming approach for source localization problems. *Digital Signal Processing* 23(2):601–609
- Choi KH, Ra WS, Park SY, Park JB (2014) Robust least squares approach to passive target localization using ultrasonic receiver array. *IEEE Transactions on Industrial Electronics* 61(4):1993–2002
- Chowdhury TJ, Elkin C, Devabhaktuni V, Rawat DB, Oluoch J (2016) Advances on localization techniques for wireless sensor networks: A survey. *Computer Networks* 110:284–305
- Coluccia A, Fascista A (2018) On the hybrid TOA/RSS range estimation in wireless sensor networks. *IEEE Transactions on Wireless Communications* 17(1):361–371. <https://doi.org/10.1109/TWC.2017.2766628>
- Cui L, Li G, Lin Q, Chen J, Lu N (2016) Adaptive differential evolution algorithm with novel mutation strategies in multiple sub-populations. *Computers & Operations Research* 67:155–173
- Das S, Mullick SS, Suganthan PN (2016) Recent advances in differential evolution—An updated survey. *Swarm and Evolutionary Computation* 27:1–30
- Deak G, Curran K, Condell J (2012) A survey of active and passive indoor localisation systems. *Computer Communications* 35(16):1939–1954
- Derrac J, García S, Molina D, Herrera F (2011) A practical tutorial on the use of nonparametric statistical tests as a methodology for comparing evolutionary and swarm intelligence algorithms. *Swarm and Evolutionary Computation* 1(1):3–18
- Destino G, Abreu G (2011) On the maximum likelihood approach for source and network localization. *IEEE Transactions on Signal Processing* 59(10):4954–4970
- Einemo M, So HC (2015) Weighted least squares algorithm for target localization in distributed MIMO radar. *Signal Processing* 115:144–150
- Goel R, Maini R (2018) A hybrid of ant colony and firefly algorithms (hafa) for solving vehicle routing problems. *Journal of Computational Science* 25:28–37
- Goyal S, Patterh MS (2014) Wireless sensor network localization based on cuckoo search algorithm. *Wireless Personal Communications* 79(1):223–234
- Grant M, Boyd S (2008) Graph implementations for nonsmooth convex programs. In: Blondel V, Boyd S, Kimura H (eds) *Recent Advances in Learning and Control*. Springer-Verlag Limited, Lecture Notes in Control and Information Sciences, pp 95–110
- Grant M, Boyd S (2014) CVX: Matlab software for disciplined convex programming, version 2.1. <http://cvxr.com/cvx>
- Guo L, Wang GG, Wang H (2013) Wang D (2013) An effective hybrid firefly algorithm with harmony search for global numerical optimization. *The Scientific World Journal*
- Halder S, Ghosal A (2016) A survey on mobile anchor assisted localization techniques in wireless sensor networks. *Wireless Networks* 22(7):2317–2336. <https://doi.org/10.1007/s11276-015-1101-2>
- Harikrishnan R, Kumar VJS, Ponnmalar PS (2016) A comparative analysis of intelligent algorithms for localization in wireless sensor networks. *Wireless Personal Communications* 87(3):1057–1069. <https://doi.org/10.1007/s11277-015-2635-4>
- Huang B, Xie L, Yang Z (2015) TDOA-based source localization with distance-dependent noises. *IEEE Transactions on Wireless Communications* 14(1):468–480
- Jiang Y, Liu M, Chen T, Gao L (2018) TDOA passive location based on cuckoo search algorithm. *Journal of Shanghai Jiaotong University (Science)* 23(3):368–375
- Kaur A, Kumar P, Gupta GP (2016) A novel DV-Hop algorithm based on gauss-newton method. 2016 Fourth International Conference on Parallel, Distributed and Grid Computing (PDGC), IEEE, pp 625–629
- Kocub B, Dey S, Sun X (2016) Strong SOCP relaxations for the optimal power flow problem. *Operations Research* 64:1177–1196
- Kuila P, Gupta SK, Jana PK (2013) A novel evolutionary approach for load balanced clustering problem for wireless sensor networks. *Swarm and Evolutionary Computation* 12:48–56
- Kulkarni VR, Desai V, Kulkarni RV (2019) A comparative investigation of deterministic and metaheuristic algorithms for node localization in wireless sensor networks. *Wireless Networks* 25(5):2789–2803
- Li Z, Chung PJ, Mulgrew B (2017) Distributed target localization using quantized received signal strength. *Signal Processing* 134:214–223
- Liang JJ, Qu BY, Suganthan PN (2013) Problem definitions and evaluation criteria for the cec 2014 special session and competition on single objective real-parameter numerical optimization. Zhengzhou University, Zhengzhou China and Technical Report, Nanyang Technological University, Singapore, Computational Intelligence Laboratory, p 635
- Lieu QX, Do DTT, Lee J (2018) An adaptive hybrid evolutionary firefly algorithm for shape and size optimization of truss structures with frequency constraints. *Computers & Structures* 195:99–112
- Lin L, So HC, Chan FK, Chan YT, Ho K (2013) A new constrained weighted least squares algorithm for TDOA-based localization. *Signal Processing* 93(11):2872–2878
- Luthra J, Pal SK (2011) A hybrid firefly algorithm using genetic operators for the cryptanalysis of a monoalphabetic substitution cipher. In: *Information and communication technologies (WICT), 2011 world congress on, IEEE*, pp 202–206
- Mohamed AW (2017) Almazayad AS (2017) Differential evolution with novel mutation and adaptive crossover strategies for solving large scale global optimization problems. *Applied Computational Intelligence and Soft Computing*
- Mohamed AW, Suganthan PN (2018) Real-parameter unconstrained optimization based on enhanced fitness-adaptive differential evolution algorithm with novel mutation. *Soft Computing* 22(10):3215–3235
- Noroozi A, Sebt MA (2015) Target localization from bistatic range measurements in multi-transmitter multi-receiver passive radar. *IEEE Signal Processing Letters* 22(12):2445–2449
- Qian W, Chai J, Xu Z, Zhang Z (2018) Differential evolution algorithm with multiple mutation strategies based on roulette wheel selection. *Applied Intelligence* pp 1–18
- Qu X, Xie L (2016) An efficient convex constrained weighted least squares source localization algorithm based on TDOA measurements. *Signal Processing* 119:142–152

- Rao SS, Rao SS (2009) Engineering optimization: theory and practice. John Wiley & Sons, New Jersey
- Sachs J (2013) Handbook of Ultra-Wideband Short-Range Sensing: Theory. John Wiley & Sons, Sensors, Applications
- Sadowski S, Spachos P (2018) RSSI-based indoor localization with the internet of things. *IEEE Access* 6:30149–30161
- Shen J, Molisch AF, Salmi J (2012) Accurate passive location estimation using TOA measurements. *IEEE Transactions on Wireless Communications* 11(6):2182–2192
- Singh SP, Sharma S (2015) Range free localization techniques in wireless sensor networks: A review. *Procedia Computer Science* 57:7–16
- Storn R, Price K (1997) Differential evolution—a simple and efficient heuristic for global optimization over continuous spaces. *Journal of global optimization* 11(4):341–359
- Tanabe R, Fukunaga A (2013) (2013) Success-history based parameter adaptation for differential evolution. *Evolutionary Computation (CEC)*. *IEEE Congress on, IEEE*, pp 71–78
- Wang G, Li Y, Ansari N (2013) A semidefinite relaxation method for source localization using TDOA and FDOA measurements. *IEEE Transactions on Vehicular Technology* 62(2):853–862
- Wang H, Cui Z, Sun H, Rahnamayan S, Yang XS (2017) Randomly attracted firefly algorithm with neighborhood search and dynamic parameter adjustment mechanism. *Soft Computing* 21(18):5325–5339
- Wang Y (2015) Linear least squares localization in sensor networks. *EURASIP Journal on Wireless Communications and Networking* 2015(1):51
- Wang Y, Wu Y (2016) An efficient semidefinite relaxation algorithm for moving source localization using TDOA and FDOA measurements. *IEEE Communications Letters* 21(1):80–83
- Wang Y, Cai Z, Zhang Q (2011) Differential evolution with composite trial vector generation strategies and control parameters. *IEEE Transactions on Evolutionary Computation* 15(1):55–66
- Wang Y, Ma S, Chen CP (2014) TOA-based passive localization in quasi-synchronous networks. *IEEE Communications Letters* 18(4):592–595
- Wu G, Shen X, Li H, Chen H, Lin A, Suganthan PN (2018) Ensemble of differential evolution variants. *Information Sciences* 423:172–186
- Wu N, Yuan W, Wang H, Kuang J (2016) TOA-based passive localization of multiple targets with inaccurate receivers based on belief propagation on factor graph. *Digital Signal Processing* 49:14–23
- Wu P, Su S, Zuo Z, Guo X, Sun B, Wen X (2019) Time difference of arrival (TDoA) localization combining weighted least squares and firefly algorithm. *Sensors* 19(11):2554
- Xu S, Doğançay K (2015) Optimal sensor deployment for 3D AOA target localization. *2015 IEEE International Conference on Acoustics, Speech and Signal Processing (ICASSP)*, *IEEE*, pp 2544–2548
- Yan J, Zhang X, Luo X, Wang Y, Chen C, Guan X (2018) Asynchronous localization with mobility prediction for underwater acoustic sensor networks. *IEEE Transactions on Vehicular Technology* 67(3):2543–2556
- Yang XS (2009) Firefly algorithms for multimodal optimization. In: *International symposium on stochastic algorithms*, Springer, pp 169–178
- Yang XS (2010a) Firefly algorithm, levy flights and global optimization. In: *Research and development in intelligent systems XXVI*, Springer, pp 209–218
- Yang XS (2010b) Firefly algorithm, stochastic test functions and design optimisation. *International Journal of Bio-Inspired Computation* 2(2):78–84, 1003.1409v1
- Zekavat R, Buehrer RM (2011) Handbook of position location: Theory, practice and advances, vol 27. John Wiley & Sons, New Jersey
- Zhang D, Fang Z, Wang Y, Sun H (2015a) Research on an improved DV-Hop localization algorithm based on PSODE in WSN. *J Commun* 10(9):
- Zhang J, Sanderson AC (2009) JADE: adaptive differential evolution with optional external archive. *IEEE Transactions on evolutionary computation* 13(5):945–958
- Zhang L, Liu L, Yang XS, Dai Y (2016) A novel hybrid firefly algorithm for global optimization. *PloS one* 11(9):e0163230
- Zhang Y, Wei D, Fu W, Yang B (2014) Target positioning with GDOP assisted nodes selection algorithm in wireless sensor networks. *International Journal of Distributed Sensor Networks* 10(6):404812
- Zhang Y, Wang S, Ji G (2015b) A comprehensive survey on particle swarm optimization algorithm and its applications. *Mathematical Problems in Engineering*

Publisher's Note Springer Nature remains neutral with regard to jurisdictional claims in published maps and institutional affiliations.